

# **Blocking the RNA interference pathway improves oncolytic virus therapy**

Submitted by: Amelia Aitken

Supervisor: Dr. John Bell

A thesis submitted to the Faculty of Graduate and Postdoctoral  
Studies in partial fulfilment of the requirements for the degree of  
Master of Science

Department of Biochemistry, Microbiology and Immunology  
Specialization in Human and Molecular Genetics

**University of Ottawa  
Faculty of Medicine  
Ottawa, Ontario, Canada**

© Amelia Aitken, Ottawa, Canada, 2017

## **Abstract**

Oncolytic viruses are novel candidates for cancer therapy and their efficacy relies on their capacity to overcome the host's anti-viral barriers. In mammalian cells, the anti-viral response involves a protein-signaling cascade known as the interferon pathway, which alerts the immune system and limits the propagation of infection. Given that most cancer cells have defects in this pathway, they are susceptible to viral infection and responsive to oncolytic virotherapy. For reasons that remain unknown, many cancers are still refractory to oncolytic viruses, which suggests the existence of additional antiviral mechanisms. In this study, we investigate the potential involvement of an alternative antiviral pathway in cancer cells. Given that insects and plants rely on the RNA silencing pathway for their anti-viral protection, we investigated the presence of a similar mechanism in cancer cells. We found viral genome-derived small RNAs in various cancer cell lines upon infection, which is indicative of an RNA-mediated antiviral response. Also, various viruses encode suppressors of the RNA interference pathway. To determine if an oncolytic virus could benefit from such a factor, we engineered an oncolytic virus variant to encode the Nodamura virus B2 protein, a known inhibitor of RNA silencing-mediated immune responses. Using this virus, we observed enhanced cytotoxicity in 33 out of the 38 human cancer cell lines tested. Furthermore, our results show inhibition of viral genome cleavage and altered microRNA processing by our B2-expressing oncolytic virus. Taken together, our data suggests the blockade of RNA silencing antiviral pathways and/or antiviral microRNA processing improves the efficacy of our B2-encoding virus in a cell-line specific manner. Overall, our results establish the improved potential of our novel virus therapy and demonstrate for the first time the involvement of RNA pathways in the antiviral defense of cancer cells.

## **Acknowledgements**

I would like to thank my supervisor Dr. John Bell for his mentorship and guidance throughout my studies. This lab and research environment has provided me with countless opportunities to learn and develop as a young scientist and for this I am eternally grateful. To Dr. Carolina Ilkow, thank you for your thoughtful input and constant support. To Dr. Marie-Claude Bourgeois-Daigneault and Dr. Dominic Roy, thank you for not only being my “go-to” mentors in the lab but for also becoming my second family. You’ve been there for me through it all and I’ll forever cherish the laughs we’ve shared. To my friends and colleagues in the Cancer Centre, I couldn’t have asked for better people to spend my days with. It’s been a pleasure. Thank you for your help, smiles and love. Lastly, to my family, thank you for always being curious about what I’m doing even though I know you don’t understand most of it. You believe in me even when I don’t believe in myself. My successes are your successes and I wouldn’t be where I am today without all of you behind me.

## List of Abbreviations

AGO – argonaute

dsRNA – double-stranded ribonucleic acid

EGFR - epidermal growth factor receptor

ESC – embryonic stem cell

hpi – hours post infection

IFN – interferon

kb – kilobases

miRNA – microRNA

MOI – multiplicity of infection

Nodamura virus – NV

OV – oncolytic virus

pre-miRNA – pre-microRNA

pri-miRNA – primary microRNA

PBS – phosphate buffered saline

PRR – pathogen recognition receptor

pfu – plaque forming unit

RISC – RNA induced silencing complex

RNAi – RNA interference

small interfering RNA – siRNA

VSV – vesicular stomatitis virus

WT – wild-type

## List of Figures

<b>Figure 1.1</b> The mammalian microRNA processing pathway.....	10
<b>Figure 3.1</b> The Nodamura virus B2 protein enhances VSV $\Delta$ 51 replication in resistant cancer cell lines.....	25
<b>Figure 3.2</b> The Nodamura virus B2 protein does not enhance replication of a number of oncolytic viruses.....	27
<b>Figure 3.3</b> B2 is expressed from the VSV $\Delta$ 51 backbone.....	30
<b>Figure 3.4</b> B2 is functional in insect cells when expressed by VSV $\Delta$ 51.....	32
<b>Figure 3.5</b> VSV $\Delta$ 51-mediated expression of B2 enhances cytotoxicity in tumor cell lines.....	35
<b>Figure 3.6</b> VSV $\Delta$ 51-B2 enhances improves viral replication in cancer cells but not healthy cells.....	37
<b>Figure 3.7</b> Growth kinetics of VSV $\Delta$ 51-B2 in resistant cancer cell lines.....	39
<b>Figure 3.8</b> VSV $\Delta$ 51-B2 alters microRNA levels in 7860s.....	42
<b>Figure 3.9</b> VSV $\Delta$ 51-B2 alters RNA processing in various cancer cell lines.....	44
<b>Figure 3.10</b> VSV $\Delta$ 51-B2 inhibits viral genome cleavage in certain cancer cell lines.....	46
<b>Figure 3.11</b> VSV $\Delta$ 51-B2 infection upregulates interferon expression.....	50
<b>Figure 3.12</b> The effects of VSV $\Delta$ 51-B2 on modulating the interferon response.....	52
<b>Figure 3.13</b> The effects of interferon pre-treatment or blocking on VSV $\Delta$ 51-B2 infection.....	54
<b>Figure 3.14</b> VSV $\Delta$ 51-B2 enhances replication within murine cell lines and tumour models.....	57
<b>Figure 3.15</b> VSV $\Delta$ 51-B2 treatment enhances serum cytokine levels in the Renca tumour model.....	59
<b>Figure 3.16</b> Biodistribution of VSV $\Delta$ 51-B2 in tumour-bearing C57BL/6 mice.....	61

## Table of Contents

<b>Abstract.....</b>	<b>ii</b>
<b>Acknowledgements.....</b>	<b>iii</b>
<b>List of Abbreviations.....</b>	<b>iv</b>
<b>List of Figures.....</b>	<b>v</b>
<b>Table of Contents.....</b>	<b>vi</b>
<b>1. Introduction.....</b>	<b>1</b>
<b>1.1 Cancer and oncolytic viruses (OVs) as novel therapies.....</b>	<b>1</b>
1.1.1 The need for novel therapies.....	1
1.1.2 OV overview.....	2
<b>1.2 Vesicular stomatitis virus (VSV).....</b>	<b>4</b>
1.2.1 VSV as an OV.....	4
1.2.2 VSV replication cycle.....	4
1.2.3 VSV $\Delta$ 51 as a safe OV platform.....	6
<b>1.3 RNA interference (RNAi) as an innate immune mechanism.....</b>	<b>8</b>
1.3.1 Overview of RNAi.....	8
1.3.2 RNAi as an anti-viral mechanism.....	11
1.3.3 Viral suppressors of RNAi.....	11
1.3.4 Antiviral RNAi in mammalian cells.....	12
<b>1.4 Hypothesis Rationale.....</b>	<b>15</b>
<b>1.5 Hypothesis.....</b>	<b>15</b>
<b>1.6 Experimental Objectives.....</b>	<b>15</b>
<b>2. Materials and Methods.....</b>	<b>16</b>
2.1 Cell lines and culture.....	16
2.2 DNA constructs and viral constructs.....	16
2.2 Generation of stable cells.....	17
2.4 Virus quantification.....	17
2.5 Virus rescue and purification.....	18
2.6 Cell Viability Assay .....	18
2.7 Western Blots.....	19
2.8 Quantitative PCR (qPCR).....	20
2.9 ELISA.....	21
2.10 Supernatant transfer experiments.....	21
2.11 IFN pre-treatment experiments.....	22
2.12 Sequencing and bioinformatics analysis.....	22
2.13 <i>In vivo</i> experiments and tumour models.....	22

<b>3. Results.....</b>	<b>24</b>
3.1 Endogenous B2 expression enhances virus production.....	24
3.2 VSV $\Delta$ 51-B2 expresses a functional B2 protein.....	29
3.3 B2 expression improves VSV $\Delta$ 51 cytotoxicity in a panel of human cancer cell lines.....	34
3.4 VSV $\Delta$ 51-B2 alters microRNA levels and prevents VSV genome cleavage in cancer cells.....	41
3.5 VSV $\Delta$ 51-B2 and the Type I IFN response.....	48
3.6 Virus-mediated B2 expression enhances tumour-specific replication and increases cytokine production.....	56
<b>4. Discussion.....</b>	<b>63</b>
4.1 A novel role for antiviral RNAi in human cancers.....	63
4.2 The controversy on mammalian RNAi.....	64
4.3 Enhanced cell killing of VSV $\Delta$ 51-B2 in human cancer cell lines.....	66
4.4 RNAi inhibition through the Vaccinia virus VSR, VP55, enhances VSV $\Delta$ 51 killing .....	67
4.5 The interplay between B2 and the IFN response.....	68
4.6 MicroRNAs and virus replication.....	70
4.7 Dicer in cancer and infection.....	72
4.8 Implications for VSV $\Delta$ 51-B2 in cancer treatment.....	73
<b>5. Concluding Remarks.....</b>	<b>74</b>
<b>References.....</b>	<b>75</b>
<b>Curriculum vitae.....</b>	<b>87</b>

## **1. Introduction**

### **1.1 Cancer and oncolytic viruses (OVs) as novel therapies**

#### **1.1.1 The need for novel cancer therapies**

In an era of modern medicine, cancer continues to be one of the most complex biological problems to challenge researchers worldwide. Approximately 2 out of 5 Canadians will develop a cancer in their lifetime and it is predicted that one quarter of them will die from the disease (Canadian Cancer Society, 2016 Statistics). Fortunately, the field of cancer therapy has seen significant progression within recent years and as a result, the outlook for cancer patients has improved. While many cancers respond well to available therapies and have a high rate of long-term remission, the treatment of late-stage disseminated disease, as well as the frequent occurrence of treatment-resistance remain challenges that are unmet by current standards of care. The quest for the development of alternative options for these patients has given rise to the development of a myriad of novel strategies. Immunotherapeutic approaches such as immune checkpoint blockade<sup>1</sup>, chimeric-antigen receptor T cells<sup>2</sup>, adoptive cell therapies<sup>3</sup>, anti-cancer vaccines<sup>4</sup>, and oncolytic viruses (OVs)<sup>5</sup> are examples of promising innovative cancer therapies.

OV therapy relies on the selection or engineering of viruses with favorable therapeutic index; viruses which specifically kill tumour cells without considerably harming normal tissues<sup>6</sup>. Importantly, OV therapies effectively address a number of concerns associated with current treatment options. The tumour-specificity of OVs limits the side-effects of treatment which comes in sharp contrast to the quality of life-compromising toxicity associated to many drugs as well as radiation therapy. OV therapies are not without side-effects however, theirs resemble flu-like symptoms including chills, nausea and fatigue and are low-grade and short-term compared to those experienced with classical therapy regimens<sup>7</sup>. In addition, the systemic infusion of OVs

allows for the treatment of micrometastases in anatomical locations that are difficult to access by localized administration techniques like radiation therapy. Recent years have seen an increasing drive for clinical testing of various OV's for cancer treatment<sup>8</sup>. OV therapy is now being tested as a monotherapy as well as in combination strategies and viral vaccine approaches.<sup>9,10</sup> With the first virus approved for patient-use by the United States Food and Drug Administration in 2015<sup>11,12</sup> and the success to-date of other OV candidates in clinical testing, the treatment should continue to improve the outlook for cancer patients and has the potential to become a popular treatment option for otherwise difficult to treat disease forms.

### **1.1.2 OV overview**

There are multiple mechanisms which contribute to the cancer-fighting abilities of OV's. The main ones are believed to be 1- the direct killing of cancer cells, 2- the destruction of tumor-associated vasculature and 3- the induction of anti-tumor immunity<sup>13,14</sup>. In order to achieve these effects, replication within the tumor bed is necessary and therefore, OV's must be able to overcome the anti-viral barriers triggered by the cancer cells as well as the tumor microenvironment following infection. The type I interferon (IFN) pathway is a well-characterized mammalian signaling cascade triggered upon viral attack to contain infection<sup>15</sup>. Type I IFNs promote an antiviral and anti-proliferative state in addition to inducing innate and adaptive immunity<sup>15</sup>. This response is necessary to the control of viral infection and thus, the safety of OV therapy. The IFN signaling cascade triggered by VSV is initiated through the stimulation of pattern-recognition receptors (PRRs)<sup>16</sup>. PRRs include Toll-like receptors (TLRs) such as TLR3, TLR4 and TLR7, as well as retinoic acid-inducible gene I (RIG-I) receptors<sup>15</sup>. PRRs recognize pathogen-associated molecular patterns (PAMPS) like viral RNA and initiate the production of IFNs and the tran-

scription of downstream IFN-stimulated-genes (ISGs)<sup>16</sup>. This initial response is induced within 3 to 6 hours of infection and leads to the induction of secondary and tertiary response genes through autocrine signaling. Together, the ISGs such as MxA<sup>17</sup>, PKR<sup>18</sup> and IFITM2/3<sup>19</sup> prevent the propagation of infection by inhibiting viral protein synthesis and inducing cell suicide.

Interestingly, the genetic alterations promoting tumorigenesis tend to make cancer cells more susceptible to viral infection<sup>20</sup>. Indeed, many of the pathways activated in response to infection to inhibit cell growth, activate apoptosis, and alert the immune system, are incompatible with malignant growth and therefore are often defective in cancer cells<sup>21</sup>. Since these defects are so common in cancers, many are quite susceptible to viral infection. For instance, the well-known tumour suppressor gene p53 functions as a host antiviral factor in addition to its more commonly known functions in promoting cell cycle arrest and apoptosis. In fact, p53 is a direct transcriptional target of Type I IFNs and promotes the rapid expression of antiviral and pro-inflammatory genes such as TNF $\alpha$ , IRF5/9, TLR3, and CCL2<sup>22</sup>. Its expression also contributes to virus-induced apoptosis and has been shown to limit replication of a number of viruses<sup>23</sup>. As another example, the tumour suppressor retinoblastoma protein Rb also contributes to the mammalian antiviral response. In fact, deletion of Rb in MEFs results in defects in activation of the antiviral NF- $\kappa$ B pathway and downstream IFN- $\beta$  production and enhances VSV replication<sup>24</sup>. This is not limited to VSV as IFNs have also been shown to augment the interaction between Rb and its binding sequence within the E1A enhancer which represses early adenovirus replication<sup>25</sup>. As somatic mutations to p53 and/or Rb are among the most common mutations in cancer, they represent just two examples of the defects characterizing cancers which also render them hypersensitive to infection and provide a basis for the use of OV's as potent, tumour-specific bio-therapeutics<sup>26</sup>.

## 1.2 Vesicular stomatitis virus (VSV)

### 1.2.1 VSV as an OV

One well characterized OV is VSV; a prototypical OV platform that is the focus of this research project. VSV is a member of the *Rhabdoviridae* family<sup>27</sup>. Rhabdoviruses are enveloped with a negative sense, single-stranded RNA genome and their natural hosts include plants, insects, and animals<sup>27</sup>. VSV has several characteristics that render it an ideal OV candidate; 1- VSV is capable of infecting and killing a wide spectrum of tumour types, 2- its rapid and robust replication facilitates effective self-amplification and enables large-scale clinical production and 3- its negative-sense RNA genome is an additional safety feature as it replicates in the cytosol and is unable to integrate into host DNA<sup>28</sup>. A multitude of VSV recombinants have been developed and characterized to date. One leading candidate which is currently in clinical development (NCT01628640) is a VSV variant encoding human IFN- $\beta$ . The expression of this anti-viral cytokine by the virus improves its safety profile and was shown to efficiently limit toxicity in various mouse models<sup>29</sup>.

### 1.2.2 VSV replication cycle

The VSV genome is 11kb-long and encodes five essential proteins known as the nucleocapsid (N), phosphoprotein (P), matrix protein (M), glycoprotein (G) and large polymerase (L)<sup>27</sup>. The infection is initiated upon attachment of the G protein, which covers the surface of the virion, to its receptor the low-density lipoprotein receptor (LDL-R)<sup>27,28</sup>. LDL-R is ubiquitously expressed and therefore, VSV is capable of infecting nearly all mammalian cells<sup>27,28</sup>. Following the binding of the virus to its receptor, internalization of the virion occurs via actin- and clathrin-mediated endocytosis<sup>27,28</sup>. Replication of the VSV genome requires the release of the ribonucleoprotein core contained within the viral envelope<sup>27,28</sup>. The acidification of internalized VSV-

containing endosomes facilitates the fusion of the viral envelope and endosomal membrane and results in the cytoplasmic release of the VSV core<sup>27,28</sup>. Within the core, the viral genome itself is encapsulated by N proteins, which form a nuclease-resistant nucleocapsid and protects the genome from degradation<sup>27,28</sup>. Replication of the genome proceeds by the VSV-encoded RNA polymerase, which is formed by P and L<sup>27,28</sup>. Viral genome transcription occurs in a gradient-fashion and results in the highest transcript levels for N, followed by P, M, G and L<sup>30</sup>. The rapid transcription of VSV transcripts allows for the assembly of viral progeny within approximately 2-3 hours following the initial infection<sup>28</sup>.

VSV has evolved to rapidly counter activation of the IFN response and one of the many functions of VSV M is to inhibit the activation of this antiviral cascade. M limits the expression of antiviral genes at the transcriptional and translational levels. In infected cells, M can be found in the nucleus where it has been shown to inhibit the function of all three host RNA polymerases<sup>31,32</sup>. M also interacts with the nucleocytoplasmic trafficking proteins Rae1 and Nup98 and prevents trafficking of cellular mRNA from the nucleus<sup>33</sup>. In addition, M has been shown to interfere with the Jak/STAT signaling pathway which prevents the activation of the secondary and tertiary IFN responses<sup>34</sup>. Overall, the wildtype VSV M effectively antagonizes the cellular antiviral response at various steps allowing the virus to infect even healthy IFN-responsive tissues.

### **1.2.3 VSV $\Delta$ 51 as a safe OV platform**

Given its efficiency at infecting most tumour types, VSV is a promising OV candidate, however, its uncontrolled replication in healthy tissues represents a major safety concern. Ideally, a VSV OV platform should retain its ability to trigger an IFN response but unlike the wild

type version of the virus, be unable to combat this response. In their 2003 publication, Stojdl *et al* describe two naturally occurring VSV variants, named AV1 and AV2, as being selectively-attenuated in healthy tissues while remaining highly cytotoxic to tumours<sup>35</sup>. AV1 and AV2 produced uncharacteristically small plaques in two infected IFN-responsive tumor cell lines, the human prostate carcinoma PC3 and renal carcinoma Caki-1 cells<sup>35</sup>. Further sequencing experiments of an isolated AV1 clone revealed a mutation in the M protein of the virus where the methionine 51 was substituted for an arginine<sup>35</sup>. This prompted the development of a VSV deletion mutant of methionine 51, known as VSVΔ51, as the deletion is more stable compared to a substitution given the rapid evolution of the virus<sup>35</sup>. Subsequent work using this VSV mutant demonstrated its improved therapeutic index that was attributed to its impaired capacity to block the IFN response<sup>35</sup>. Unlike wildtype VSV, which induces transcription of ISGs but blocks their nuclear export, VSVΔ51 infection allows for the cytoplasmic translocation of induced genes and therefore the production of IFNs<sup>35</sup>. The resulting robust antiviral response is capable of protecting IFN-responsive cells from infection. The attenuated profile of VSVΔ51 in healthy tissues does not however impair its oncolytic potential given the known defects of tumor cells in innate immune pathways<sup>35</sup>. In fact, the *in vivo* systemic administration of VSVΔ51 is a highly effective therapy in murine tumour models with impaired IFN signaling, including the aggressive CT26 colon carcinoma model<sup>35</sup>. It is important to note that these defects vary among cancers and despite its broad efficacy, the efficacy of VSVΔ51 treatment varies accordingly<sup>36</sup>. While a specific cell line's capacity to produce IFN is an important factor when it comes to virus-sensitivity *in vitro*, the potent response triggered by cells from the tumor microenvironment as well as immune cells further complicate the *in vivo* efficacy of OV therapy. Despite this, the responsiveness sta-

tus of each cancer is undoubtedly an important factor which influence the therapeutic efficacy of VSVΔ51 treatment.

As an additional safety feature, the tropism of VSV can be modulated to direct tissue-specificity. One way to alter VSV tropism is through the addition of microRNA target sequences directly into the virus genome<sup>37</sup>. This ensures that VSV replication is blocked in tissues expressing the complementary microRNA as it leads to repression of genome replication or direct cleavage<sup>37</sup>. This is an appealing approach given that VSV has been shown to be neuropathogenic in mice and nonhuman primates and therefore, controlling its ability to infect neural cells is an important consideration<sup>38,39</sup>. For example, a VSV variant encoding the target sequence for a brain-specific microRNA, mir-125, has been shown to retain its oncolytic efficacy *in vivo* without causing neuropathogenesis, even when administered intracerebrally<sup>40</sup>.

Beyond the scope of safety, VSV can also be engineered to encode transgenes aimed at enhancing or modifying its oncolytic or immune-stimulating properties. Numerous VSV variants are reported in the literature such as those encoding tumour antigens, cytotoxic proteins, cytokines or other factors<sup>41-47</sup>. These VSV variants demonstrate the flexibility of the VSV platform and how small modifications can further enhance treatment efficacy. Most importantly, their promising pre-clinical success further emphasizes the potential for the clinical translation of highly effective VSV-based therapies.

### **1.3 RNA interference (RNAi) as an innate immune mechanism**

#### **1.3.1 Overview of RNAi**

RNA silencing is a process which is widely conserved from plants to mammals. It is well-known for its function in silencing gene expression but also has important roles in altering heterochromatin structure<sup>48</sup> and defense against transposable elements<sup>49</sup>, as well as functions as an

innate immune mechanism in certain cell types<sup>50</sup>. The concept of RNAi has been extensively studied since its initial discovery in the model organism *C. elegans*. In their 1998 publication, Fire *et. al.* were the first to propose a role for RNA in regulating transcript expression by demonstrating the selective degradation of specific *C. elegans* mRNAs through the introduction of complementary long double-stranded RNA (dsRNA)<sup>51</sup>. Since then, we have gained a thorough understanding on the mechanism and roles of RNAi in regulating cellular processes. Also, the closely related microRNA processing pathway is used by the majority of eukaryotic cells to modulate gene expression<sup>52</sup>.

The mammalian biogenesis pathways for small interfering RNAs facilitates the production of abundant levels of regulatory RNAs in response to cellular signals<sup>53,54</sup>. MicroRNA (miRNA) biogenesis begins with the transcription of genome-encoded primary miRNA (pri-miRNA) (See Fig 1.1)<sup>54</sup>. Following transcription by RNA polymerase II, a region of the pri-miRNA adopts a characteristic stem-loop structure through complementary regions and a 60-70nt fragment, including this intermediate stem-loop, is processed from the transcript by the nuclear enzyme Drosha and its co-factor DGCR8<sup>54,55</sup>. This cleavage occurs at the stem and releases the stem-loop from the primary transcript producing an RNA fragment known as a pre-miRNA<sup>54,55</sup>. Following their nuclear export, pre-miRNAs are cleaved near the loop by the cytoplasmic enzyme Dicer, which results in a mature short regulatory miRNA of approximately 22 nucleotides (nt)<sup>54,55</sup>. Endogenously-encoded siRNAs, such as those encoded in plants and insects, and synthetic exogenously supplied dsRNAs used for targeted gene knock-downs are also processed by Dicer<sup>55</sup>. Dicer-processed miRNAs and siRNAs are then loaded onto an argonaute (AGO) protein where a single strand is kept as a guide strand and the other is degraded<sup>56</sup>. The AGO-guide RNA complex, together with Dicer and other co-factors, forms the RNA Induced Silencing Complex

(RISC)<sup>56</sup>. RISC binds target transcripts via its loaded complimentary RNA and supresses messenger RNA translation when bound to AGO1, AGO3 or AGO4, or results in direct transcript cleavage when bound to the only endonuclease AGO, AGO2<sup>56,57</sup>.

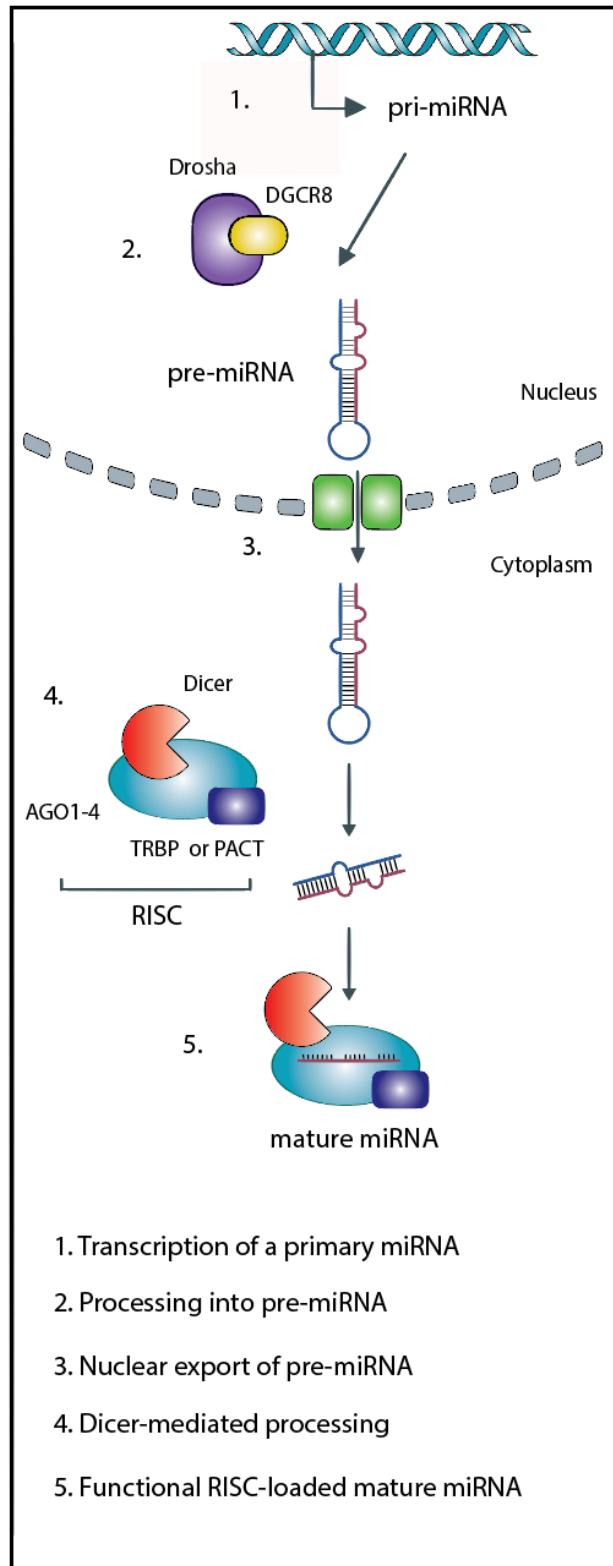


**Figure 1.1 The mammalian microRNA processing pathway.**

### **1.3.2 RNAi as an anti-viral mechanism**

Infection by RNA viruses leads to the production of viral dsRNAs which in most cell types, activates antiviral signalling cascades. As mentioned earlier (section 1.1.2), in mammalian cells, the PRRs MDA-5, RIG-I and TLR-3, recognize these viral dsRNAs which leads to the initiation of the type I IFN antiviral response<sup>58</sup>. In contrast to this mammalian system, plants, insects and invertebrates use an alternative antiviral strategy which is triggered by the recognition of viral dsRNAs by Dicer<sup>59</sup>. This RNA-initiated immune system is similar to the microRNA processing pathway used by eukaryotes. Again, viral dsRNAs are generated following infection through replication of the viral genome and can also be formed within homologous regions of viral transcripts<sup>59</sup>. As in miRNA processing (section 1.3.1), these viral dsRNAs are bound and cleaved by the host cytoplasmic enzyme Dicer, or a Dicer-homologue, to form approximately 22 nt RNA fragments<sup>59</sup>. In plants, these primary small RNAs can be replicated by RNA dependent RNA polymerases and incorporated into RNAi pathway to amplify even further this response<sup>59</sup>. Similar to previously described RNA-processing pathways, these small virally-derived RNAs are loaded into RISC to target homologous viral RNA and therefore prevent the replication and translation of viral genomes<sup>59</sup>.

### **1.3.3 Viral suppressors of RNAi**

Given the importance of RNAi-based immunity, many plant and insect viruses have evolved to counteract this pathway and encode factors called viral suppressors of RNAi (VSRs)<sup>60</sup>. A range of VSRs have been described with various mechanisms of action to combat antiviral RNAi. One common mechanism is to bind dsRNA fragments to prevent Dicer-mediated processing and subsequent gene silencing<sup>60</sup>. Another mechanism of action is the direct binding to

viral genome-targeting siRNAs that can be generated upon infection<sup>60</sup>, which blocks the loading onto RISC and prevents genome cleavage<sup>60</sup>. A good example of this is P19, a VSR encoded by the tomato bushy stunt virus and the carnation Italian ring spot virus<sup>61</sup>. Other VSRs function through binding to or inhibiting the function of AGO proteins<sup>56</sup>. An example of a VSR with this mechanism is the poliovirus P0 protein which interacts with AGO1 and ultimately promotes its degradation to limit RISC assembly<sup>62</sup>. A focus of this research project is B2, one of the most studied VSRs, encoded by the Nodamura virus (NV) from the *Nodaviridae* family<sup>63</sup>. NV is a single-stranded RNA virus which primarily infects insects but is also highly virulent to certain mammals including suckling mice and hamsters<sup>64,65</sup>. B2 binds dsRNAs as well as siRNAs corresponding to Dicer products<sup>66</sup>. As a result, B2 is able to efficiently suppress the RNAi response through inhibiting Dicer-processing of the viral genome and therefore also prevent the production of anti-viral siRNAs<sup>63</sup>. Additionally, the ability of B2 to bind siRNAs directly suggests the sequestering of viral siRNAs may be important second line defense in blocking the RNAi response of NV-infected host cells. Taken together, these examples demonstrate that ultimately, RNAi inhibition can be achieved by VSRs with diverse functions and interactions at various steps within the pathway.

#### **1.3.4 Antiviral RNAi in mammalian cells**

RNAi- and protein-mediated immunity were long thought to be non-overlapping mechanisms, with insects and invertebrates using the former strategy and mammals using the latter. In line with this, the IFN system is absent in most organisms which use antiviral RNAi to control virus infection<sup>67</sup> but whether mammalian cells rely exclusively on the IFN system is not quite as clear. Interestingly, a number of mammalian viruses encode VSRs. These viruses include Influenza<sup>68,69</sup>, Ebola<sup>70,71</sup>, Human Immunodeficiency Virus-1<sup>72,73</sup> and Vaccinia virus<sup>74</sup>. Similar to in-

sect VSRs, mammalian VSRs bind to dsRNAs and interfere with their processing. This suggests that perhaps these mammalian viruses may have encountered RNA-mediated antiviral pressure in order to evolve strategies to counter-attack this host defense mechanism. These unanswered questions have resulted in multiple groups investigating the potential for mammalian antiviral RNAi. Initial studies in mammalian somatic cells failed to detect any evidence of a RNA-mediated innate immune response. While insect cells are capable of processing transfected long dsRNAs into functional siRNAs, mammalian somatic cells do not possess this capacity<sup>75</sup>. Additionally, deep-sequencing of mammalian cell lines infected with various viruses was unable to detect significant levels of viral siRNAs<sup>76</sup>. Together, this data suggests that mammalian somatic cells do not have the capacity to process exogenous RNA into siRNAs, nor do they rely on RNA-mediated mechanisms to control viral infection.

Despite the lack of an RNAi response in somatic mammalian cells, a number of recent indications suggest that RNA-mediated antiviral responses may in fact be functional in some specific subsets of mammalian cells like in multipotent mammalian cell lineages such as germ and embryonic stem cells. Using a transgenic mouse model where Dicer-dependent siRNAs are endogenously expressed in mouse oocytes but not somatic cells, a robust RNAi response was detected in oocytes<sup>77</sup>. This suggests that the pathways required for Dicer processing of siRNAs is functional in certain pluripotent cell lineages<sup>77</sup>. Furthermore, another group has shown that the introduction of long dsRNA into murine embryonic cells results in sequence-specific gene silencing<sup>75</sup>. This was shown to induce the production of siRNAs of approximately 22nt and to be Dicer-dependent, which are features consistent with a conventional RNAi response<sup>75</sup>. The ability to effectively process long dsRNA into functional siRNAs suggests that mammalian embryonic cells have the machinery required to mount an antiviral RNAi response and multiple research

groups investigated this possibility. In 2013, Maillard *et al* investigated the changes in RNA populations in mammalian embryonic cells in response to infection with EMCV and NV<sup>78</sup>. Their results demonstrate that EMCV infection of mouse embryonic stem cells (ESCs) leads to the appearance of viral genome degradation fragments that were detectable by both deep sequencing and northern blotting<sup>78</sup>. Furthermore, those fragments were approximately 22nt and phased by 2nt a feature that indicates Dicer-processing<sup>78</sup>. This was further confirmed using Dicer-negative ESCs where those fragments were no longer detectable<sup>78</sup>. In addition to this, Maillard *et al* investigated the response to NV infection in mammalian ESCs. They demonstrate that mouse embryonic fibroblasts (MEFs) are highly susceptible to NV infection while a NV variant lacking B2 was unable to replicate<sup>78</sup>. NV cleaved genome fragments were not detectable in MEFs infected with NV but were readily detectable following infection with the B2 deletion mutant<sup>78</sup>. These genome fragments were once again detected by both deep sequencing and northern blotting and shared the characteristic features indicative of a Dicer-dependent processing<sup>78</sup>. Supporting these findings, Li *et al* demonstrated abundant production of NV-derived siRNAs in the tissues of suckling mice, which lack an IFN response and those were observed only upon disruption of B2 function<sup>79</sup>. Additionally, viral siRNA levels inversely correlate with NV replication in support of their role in controlling viral replication<sup>79</sup>. All together, these groups demonstrate for the first time the activation of a classical RNAi response to infection in undifferentiated mammalian cells. It is important to note that the IFN pathway is non-functional in both mouse oocytes and embryonic stem cells, another feature that is shared with various cancers<sup>80</sup>. Given that many cancers share common transcriptional signatures with mammalian pluripotent cells<sup>81-84</sup>, we questioned whether RNAi may also function as an alternative antiviral mechanism in malignant cells.

## **1.5 Hypothesis Rationale**

Despite showing impressive efficacy in a number of cancer models, the degree of susceptibility to VSV $\Delta$ 51 varies among human cancers, suggesting that additional antiviral mechanisms may exist within resistant tumours.

Considering 1) the discovery of mammalian antiviral RNAi in undifferentiated cells and 2) the genetic commonalities between cancer cells and undifferentiated cells, we predict that RNAi functions as a key anti-viral defense mechanism in cancer cells.

## **1.6 Hypothesis**

Antiviral RNAi functions in certain cancer cells and inhibition of RNAi could improve the efficacy of OV therapy.

## **1.7 Objectives**

1. To determine the effects of B2 expression on VSV $\Delta$ 51 killing
2. To construct and characterize a recombinant VSV $\Delta$ 51 variant encoding B2
3. To examine the mechanism by which B2 functions when produced by VSV $\Delta$ 51

## **2. Materials and Methods**

### **2.1 Cell lines and culture**

All cell lines were purchased from the American Type Culture Collections (Manassas, VA). Mammalian cells were cultured in Dulbecco's modified Eagle's medium (DMEM) (Corning cellgro, Manassas, VA) or RPMI-1640 (K562, OVCAR3, OVCAR4, OVCAR8) (Corning cellgro, Manassas, VA) supplemented with 10% fetal bovine serum (FBS) (Sigma life science, St-Louis, MO) and maintained at 37°C with 5% CO<sub>2</sub>. *Drosophila melanogaster* Schneider line 2 (S2) cells were cultured in SF900II serum-free medium (Invitrogen) at 25 °C under atmospheric pressures.

### **2.2 DNA constructs and viral constructs**

The pcDNA3.1-puro Nodamura B2 plasmid used for generating the B2 stable cell lines was made available by the Christopher Sullivan lab (Addgene plasmid # 17228)<sup>85</sup>. The pEGFP-N1 plasmid (Catalog # 6085-1) was purchased from Clontech (Mountain View, CA).

The B2 gene was amplified by PCR of the NV genome. The primers were designed to include the XhoI and NheI restriction sites as well as to insert a 6X histidine tag at the 5' end of the B2 sequence. The digested PCR fragment was cloned into the XhoI and NheI digested VSVΔ51 backbone, as previously described<sup>41</sup>. The sequences of the primers used for of B2 into the VSV backbone were as follows: forward: TATTCTCGACATGCATCATCACCACCAC-CATACAAACATGTCATGCGCTTAC, reverse: ATTTGCTAGCATCACTCATTACCAC-GCCC.

VP55 was PCR amplified from the Copenhagen strain of vaccinia virus and subcloned into pcDNA3.1 with an N-terminal Flag epitope. Flag-VP55 was subsequently PCR amplified and cloned into VSV $\Delta$ 51M using the same strategy.

### **2.3 Generation of stable cells**

M14 and 7860s were transfected using Lipofectamine 2000 (Invitrogen, Carlsbad, CA) according to manufacturer protocols. Briefly, cells were plated in 6 well format 1 day prior to transfection. Plasmid and Lipofectamine reagent were incubated for 20 mins and then added to plated cells in OptiMEM (Thermoscientific, Waltham, MA). Twenty-four hours following transfection, medium was replaced by DMEM with 10% FBS and cultured for 48 hours. Cells were then subjected to drug selection by the addition of Geneticin (800ug/mL) (Thermo Fisher, Carlsbad, CA). Cells were expanded and GFP- or YFP-positive cells were FACS-sorted twice (MoFlo Astrios).

### **2.4 Virus quantification**

Viral titers were obtained by plaque assays. Serial dilutions of the samples were prepared in serum-free DMEM. The dilutions were then transferred to monolayers of Vero cells and incubated at 37°C for 1 hour. After the incubation, cells were overlaid with 0.5% agarose in DMEM supplemented with 10% FBS. Plates were incubated for 24 hours at 37°C with 5% CO<sub>2</sub> and plaques were counted.

## **2.5 Virus rescue and purification**

Virus rescues were performed as previously described<sup>86</sup>. Vero cells were infected with T7 polymerase-expressing vaccinia virus at an MOI of 3. Following a 2 hours incubation, media was removed and cells were transfected with T7-driven plasmids encoding VSV N, P, and L genes as well as the VSVΔ51-B2 backbone. The supernatants were collected 48 hours post-transfection and passed through a 0.22 μm filter (MillexGP, Carrigtwohill, Ireland) to remove vaccinia virus.

For expansion and purification of the viral preparations, Vero cells were infected at an MOI of 0.001 and culture supernatants were collected 24h post-infection. Supernatants were then filtered through a 0.2 μm bottle top filter (Millipore, Etobicoke, Canada) and centrifuged at 30,100 g for 90 minutes. The supernatant was discarded and the pelleted virus was resuspended in Dulbecco's phosphate-buffered saline (Corning cellgro, Manassas, VA). Aliquots of purified virus was kept at -80°C.

## **2.6 Cell Viability Assay**

Relative metabolic activity of cells was used as a readout of cell viability and was determined using alamarBlue reagent (Bio-Rad, Mississauga, Ontario, Canada). The assays were performed according to manufacturer's protocol. In summary, cells were plated in 96-well plates and infected with the different viruses 24 hours later. 48 hours after virus infection, the alamarBlue reagent was added to each well to a final concentration of 1:10. The samples were incubated 1-5h and the fluorescence readings (excitation and emission wavelengths of 530nm and 590nm, respectively) were taken using a Fluoroskan Ascent FL (Thermo LabSystems, Beverly, MA).

## 2.7 Western Blots

Cell pellets were lysed on ice for 30 minutes using complete protease inhibitor cocktail (Roche, Mississauga, Ontario, Canada) supplemented lysis buffer (1% NP40, 150mM NaCl, 5mM EDTA, 50mM Tris pH 7.4). Lysates were centrifuged for 10 minutes at 16,000g and cleared supernatants were mixed with dithiothreitol-supplemented loading buffer (250 mM Tris-HCl pH 6.8, 10% SDS, 30% glycerol, 5%  $\beta$ -mercapitoethanol, 0.02% bromophenol blue). The samples were migrated on Bio-Rad Mini Protean 4-15% TGX Protein Gels (Bio-Rad, Mississauga, ON) and transferred onto PVDF membranes (GE Healthcare, Buckinghamshire, UK) prior to blocking with 5% skim milk powder (Oxoid Ltd, Basingstoke, UK) in tris-buffered saline (TBS) with 0.1% Tween-20. The membranes were probed using specific rabbit antibodies for 6X His-tag- (Abcam, Cambridge, UK), VSV (polyclonal anti-VSV serum for hyperimmune rabbits)<sup>87</sup>. Rabbit anti-GAPDH (Abcam, Cambridge, UK) and rat anti-tubulin (Novus Biologicals, Oakville, ON) antibodies were used as loading controls. Membranes were then probed with a horse radish peroxidase-coupled goat anti-rabbit secondary antibody (Millipore, Etobicoke, Canada) or goat anti-rat secondary antibody (Life Technologies, Carlsbad, CA) and the signal was revealed using Amersham ECL Western Blotting Detection Reagent (GE Healthcare, Buckinghamshire, UK). The gels were analyzed using FluorChem FC2 (Alpha Innotech, San Leandro, CA).

## 2.8 Quantitative PCR (qPCR)

For miRNA qPCRs, RNA was extracted from infected cell pellets using TRIzol reagent (Life Technologies, Carlsbad, CA) according to the manufacturer's protocol. The RNA concentration and purity was assessed using a NanoDrop ND-1000 spectrophotometer (Thermoscientific, Waltham, MA) prior to reverse transcription using Quanta microRNA cDNA synthesis kit (Gaithersburg, MD). For all other qPCRs, RNA was extracted using RNAeasy RNA extraction kit (QIAGEN, Toronto, ON, Canada) according to the manufacturers protocol. The RNA concentration and purity was assessed using a NanoDrop ND-1000 spectrophotometer (Thermoscientific, Waltham, MA) prior to reverse transcription using RevertAid H Minus First Strand cDNA Synthesis kit (Thermoscientific, Waltham, MA). miRNA qPCR primers used in this study: hsa-mir24-1-5p: TGCCTACTGAGCTGATATCAGT, hsa-mir93-5p: CAAAGTGCTGTTCGTGCAGGTAG, hsa-mir378-3p: ACTGGACTTGGAGTCAGAAGGC, hsa-mir125a-5p: TCCCTGAGACCCTTTAACCTGTGA, hsa-mir142-5p: CATAAAGTAGAAAGCACTACT, hsa-mir155-5p: TTAATGCTAATCGTGATAGGGGT, hsa-let7a-5p: TGAGGTAGTAGGTTGTATAGTT, hsa-mir16-5p: TAGCAGCACGTAAATATTGGCG, hsa-mir31-5p: AGGCAA-GATGCTGGCATAGCT, hsa-mir1-3p: TGGAATGTAAAGAAGTATGTAT, hsa-mir196b-5p: TAGGTAGTTTCCTGTTGTTGGG, hsa-mir146a-5p: TGGAATGTAAAGAAGTATGTAT, hsa-mir423-5p: TGAGGGGCAGAGAGCGAGACTTT, hsa-mir128-3p: TCACAGTGAACCGGTCTCTTT, hsa-U6: GTGCTCGCTTCGGCAGCACATATA. qPCR primers for IFN pathway genes: IFN- $\beta$ -F: CTCTCCTGTTGTGCTTCTCC, IFN- $\beta$ -R, GTCAAAGTTCATCCTGTCCTTG, OAS1-F: AAAGTGGTAAAGGGTGGCTC, OAS1-R: GCTGTCTCCTAATTCCTGG, MxA-F: GTGCATTGCAGAAGGTCAGA, MxA-R: CTGGTGATAGGCCATCAGGT. qPCR primers for GAPDH: F: ACACATTGGGGGTAG-

GAACA, R: AACTTTGGCATTGTGGAAGG. For the qPCR, Quanta Perfecta SYBR Green Fastmix (Beverly, MA) was used according to manufacturer's protocol and the samples were analyzed using a Rotor-Gene RG3000A (Corbett Research, Mortlake, Australia). U6 or GAPDH were used as the house-keeping controls for microRNA or RNA transcript qPCRs, respectively. To calculate  $\Delta\Delta Ct$ , the average GAPDH Ct from mock samples was subtracted from the Ct value for the target of interest in the same samples (control delta). The Ct values for GAPDH Ct from the experimental samples were subtracted from the Ct value for the target of interest in the same experimental samples (experimental delta). Control delta was subtracted from experimental delta and the resulting  $\Delta\Delta Ct$  value was input into the formula  $2^{-\Delta\Delta Ct}$  to obtain a final  $\Delta\Delta Ct$  value. For microRNA qPCRs,  $\Delta\Delta Ct$  was calculated as above using U6 in place of GAPDH.

## **2.9 ELISA**

The concentration of IFN- $\beta$  was determined using the human IFN-  $\beta$  ELISA kit (R&D Systems, Minneapolis, MN) according to the manufacturer's protocol.

## **2.10 Supernatant transfer experiments**

Vaccinia stocks were propagated in U2OS cells and cell-associated virus was collected by repeat (3) freeze–thaw cycles. Further purification of viral stocks was done by centrifugation at 20,700  $\times g$  through a 36% sucrose cushion (in 1 mM Tris) before resuspension in 1 mM Tris, pH 9.

To generate infected cell conditioned media, U2OS cells were either mock treated or infected with VVdd- mCherry at a multiplicity of 10 PFU/cell for 24 h, harvested and then pelleted by centrifugation. Supernatants were collected and passed through a 0.22  $\mu m$  filter to eliminate cell-free vaccinia virions. To test for factors enhancing VSV infectivity, tumor cell monolayers

were pre-treated for 2 h with conditioned U2OS supernatant. Tumor cells were then infected with VSV in the presence of conditioned medium.

### **2.11 IFN pre-treatment experiments**

Cells were plated following standard tissue culture protocol and treated with 50 IU/mL Universal Type I Interferon (PBL Assay Science, Piscataway, NJ) for 4 hours prior to infection.

### **2.12 Sequencing and bioinformatics analysis**

Small RNA was extracted from cell culture samples using TRIzol reagent (Life Technologies, Carlsbad, CA) according to manufacturer's protocol. Libraries of total small RNAs from cell culture were constructed using NEBNext Small RNA library preparation kit following the manufacturer's protocol (Ipswich, MA). Libraries were prepared and sequenced by The Centre for Applied Genomics (Hospital for Sick Children, Toronto, ON). Sequencing was done as single read 50-bases using Illumina HiSeq 2500. For the analysis, small RNA reads were trimmed to remove adaptor sequences and mapped to a VSV reference genome (NC\_001560). Mapped reads were reformatted to sort into positive and negative strand mapping reads and then to determine the size and length reads.

### **2.13 *In vivo* experiments and tumour models**

6-8 weeks old female Balb/c or nude mice (Charles River Laboratories, Wilmington, MA) were used. For the Balb/c mice  $5 \times 10^5$  Renca tumour cells were implanted subcutaneously 21 days prior to treatment. For the nude mice  $1 \times 10^8$  M14 tumor cells were implanted subcutaneously 14 days prior to treatment. A single intratumoral injection of  $1 \times 10^8$  PFU of VSV $\Delta$ 51-GFP or VSV $\Delta$ 51-B2 was performed. Tumours were harvested 24 h post-treatment, weighed and homogenized in PBS using a Powergen 125 tissue homogenizer (Fischer Scientific, Hampton, New Hampshire). Serial dilutions of tumour homogenates were titered to obtain intratumoural titer

data. For biodistribution experiments, naïve Balb/c mice were treated with a single intravenous injection of  $1 \times 10^8$  PFU of VSV $\Delta$ 51-GFP or VSV $\Delta$ 51-B2. Mice were sacrificed 24h or 48h post-treatment and organs were harvested, frozen and homogenized in PBS as above. All experiments were approved by the University of Ottawa animal care and veterinary services (ME-2258).

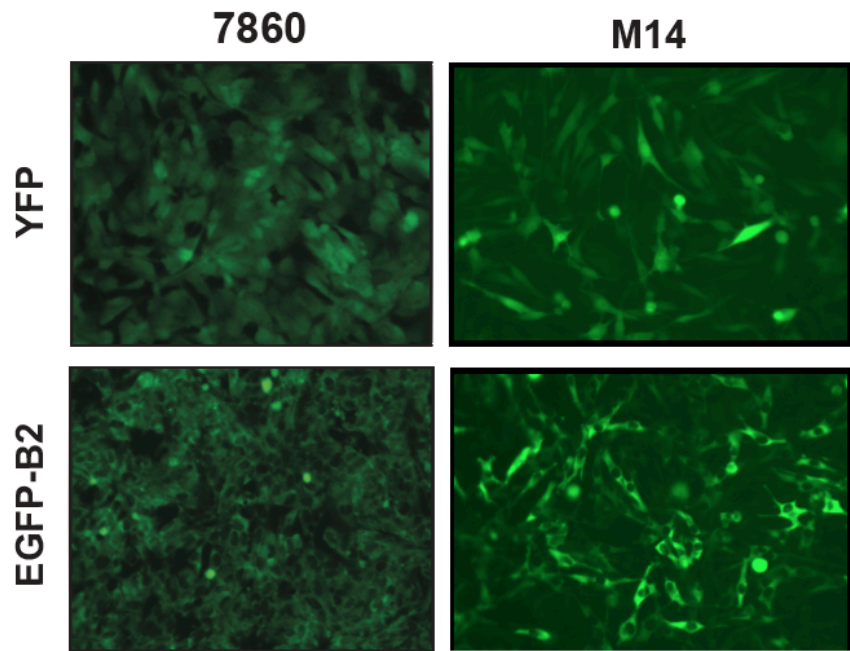
Blood collection for cytometric bead assays was done using lithium-heparin-coated capillary tubes (Sarstedt, Newton, NC). Samples were kept at room temperature and centrifuged at 16,000g for 5 minutes to collect the serum. Concentrations of IFN $\gamma$ , TNF $\alpha$ , CCL2 and IL-6 were determined using the cytometric bead array (BD Biosciences) according to the manufacturer's protocol on a Cyan ADP flow cytometer.

### **3. Results**

#### **3.1 Endogenous B2 expression enhances virus production**

To determine whether B2 expression could enhance VSV $\Delta$ 51 replication in cancer cells, we first generated cells that stably expressed B2. To do so, we transfected two VSV-resistant human cancer cell lines (M14 and 7860) with plasmids encoding either YFP as a control or an eGFP-B2 fusion construct. Fluorescence microscopy images taken upon sorting of the cells confirmed successful generation of the stable cell lines (Fig 3.1A). To determine if B2 expression could improve virus production, the stable cells were infected with VSV $\Delta$ 51 and the viral output was quantified by plaque assay 24 hours post infection (hpi). The outputs obtained from both M14-B2 and 7860-B2 stable cell lines were 10 to 100 fold higher relative to their respective control cell lines (Fig 3.1B). Interestingly, this enhancement in virus production appeared to be specific to VSV $\Delta$ 51 as no increase in virus production was observed when assessing a panel of other OVs (Fig 3.2).

**a**



**b**

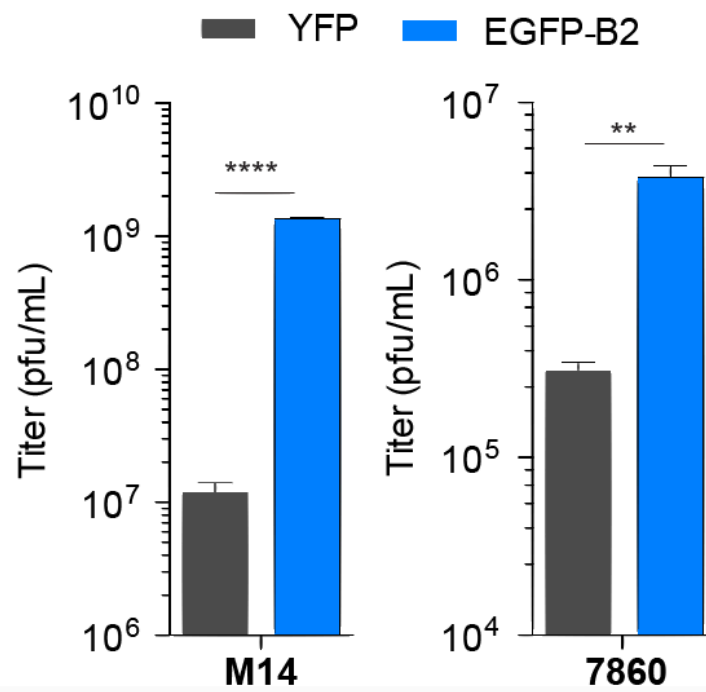


**Figure 3.1 The Nodamura virus B2 protein enhances VSV $\Delta$ 51 replication in resistant cancer cell lines.** (A) Fluorescence microscopy images of YFP or EGFP expression in M14 or 7860 cell lines stably transfected with YFP or EGFP-B2. (B) Virus concentration of supernatants of GFP- or EGFP-B2-stable M14 or 7860 cell infected with VSV $\Delta$ 51 at an MOI of 0.1 for 24h. NS:  $P > 0.1$ , \* $P < 0.1$ , \*\* $P < 0.01$ , \*\*\* $P < 0.001$  (unpaired one-tailed T-test). Only significantly different pairs are indicated on the figure.

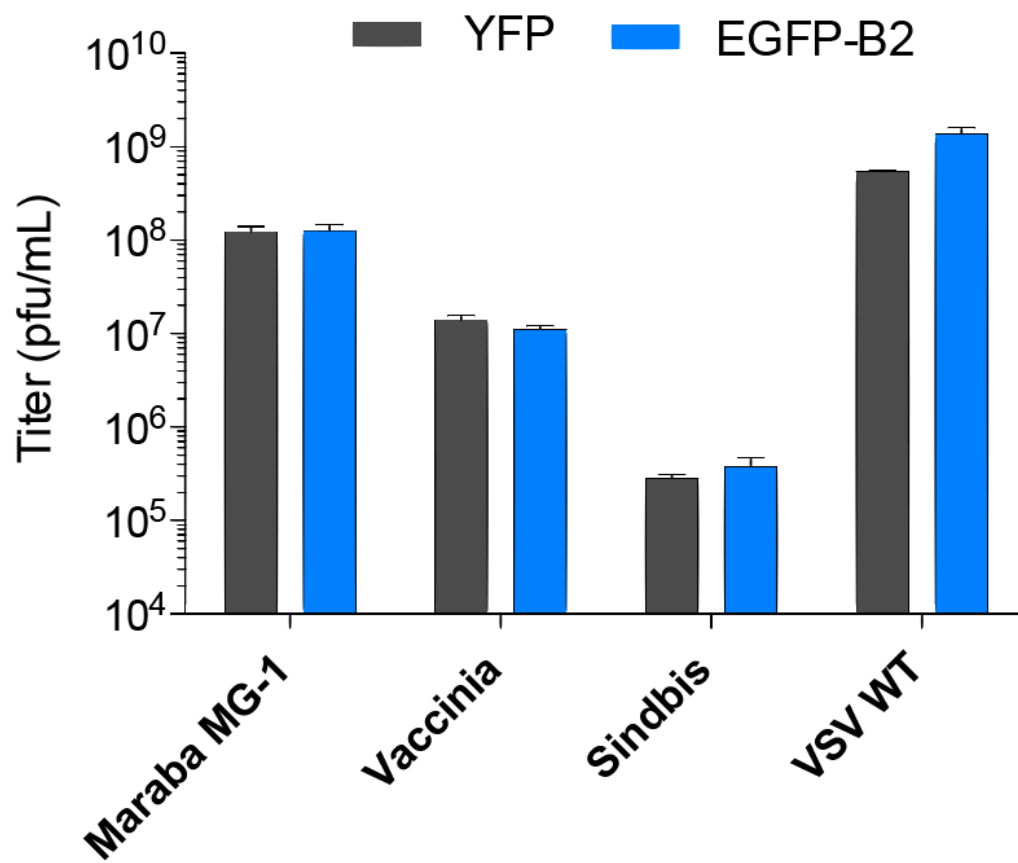


**Figure 3.2 The Nodamura virus B2 protein does not enhance replication of a number of oncolytic viruses.** Virus concentration of supernatants of GFP- or EGFP-B2-stable M14 or 7860 cell infected with MG-1, Vaccinia, Sindbis or VSV WT. Cells were infected for 24h at the following MOIs chosen based on the infectivity of the virus used; for MG-1 an MOI of 0.1, Vaccinia 0.01, Sindbis 10, and VSV WT 0.1. NS:  $P > 0.1$ , \* $P < 0.1$ , \*\* $P < 0.01$ , \*\*\* $P < 0.001$  (unpaired one-tailed T-test). Only significantly different pairs are indicated on the figure.

### **3.2 VSV $\Delta$ 51-B2 expresses a functional B2 protein**

As B2 enhanced VSV $\Delta$ 51 titers in both M14 and 7860 cell lines when endogenously expressed by the cells, we sought to determine if virus-mediated expression of B2 could have similar effects. To do so, we engineered a VSV $\Delta$ 51 virus variant encoding a His-tagged version of B2. B2 was cloned between the G and L genes of the VSV $\Delta$ 51 backbone (Fig 3.3A) since it was previously demonstrated that this location could support expression of transgenes without impairing virus replication<sup>35,41</sup>. To confirm transgene expression, Vero cells were infected with VSV $\Delta$ 51-B2 and western blots were performed on cell lysates 48 h later. The results show a band specific to B2 in the VSV $\Delta$ 51-B2 samples, which is absent in the control virus condition while VSV proteins could be detected in both samples (Fig 3.3B). We then confirmed the functionality of the virally-expressed B2 using S2 Drosophila cells, given that insect cells rely on the RNAi pathway for their antiviral defense. The viral outputs obtained from S2 cells were significantly higher for VSV $\Delta$ 51-B2 compared to VSV $\Delta$ 51-GFP at all time-points tested (Fig 3.4A). This was further supported by western blot analysis of infected S2 cells which showed increased viral proteins detected for VSV $\Delta$ 51-B2 48 hpi (Fig 3.4B).

**a**

VSV $\Delta$ 51-GFP



VSV $\Delta$ 51-B2



**b**

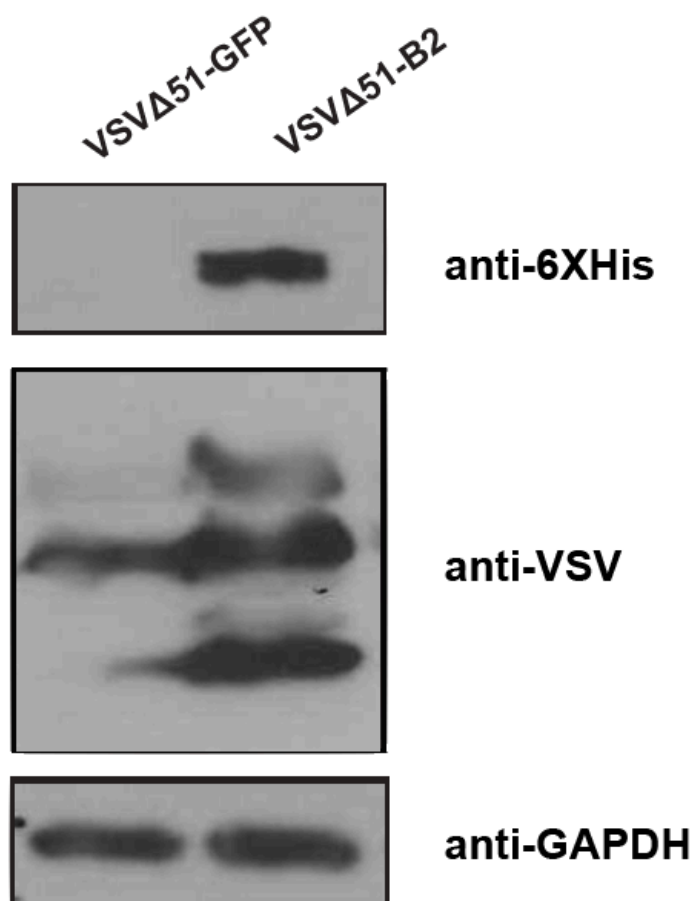


**Figure 3.3 B2 is expressed from the VSV $\Delta$ 51 backbone.** (A) Schematic representation of the VSV $\Delta$ 51-B2 and VSV $\Delta$ 51-GFP viral backbones. (B) Western blot analysis of Vero cells infected at an MOI of 1 with VSV $\Delta$ 51 or VSV $\Delta$ 51-B2 for 24h. The membranes were probed for VSV proteins, His-tagged B2 and GAPDH.

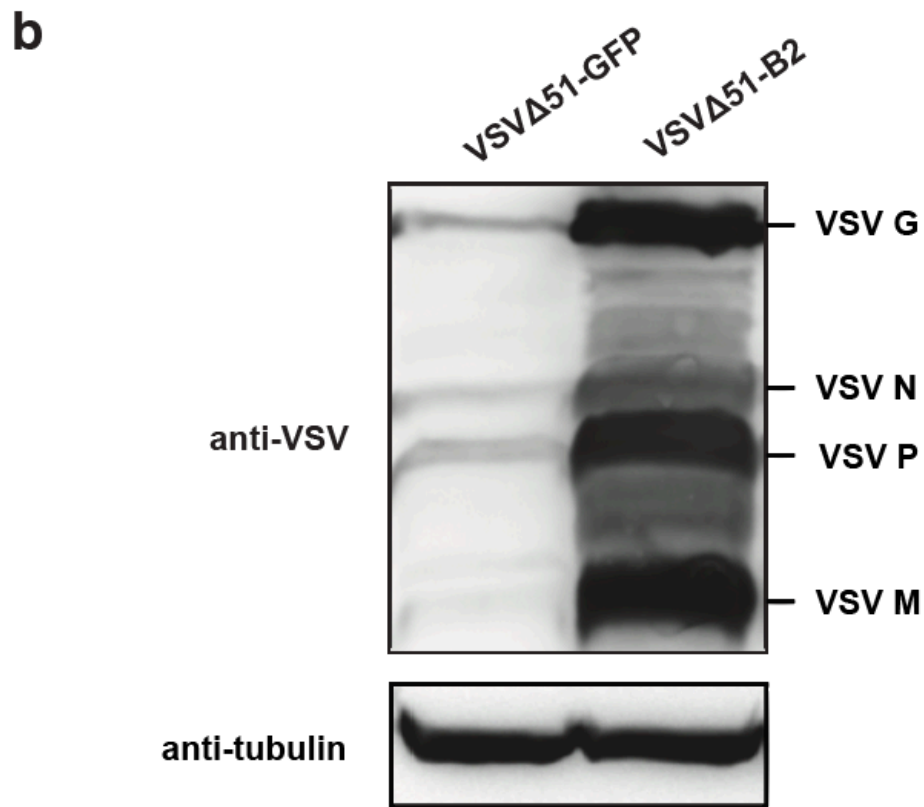
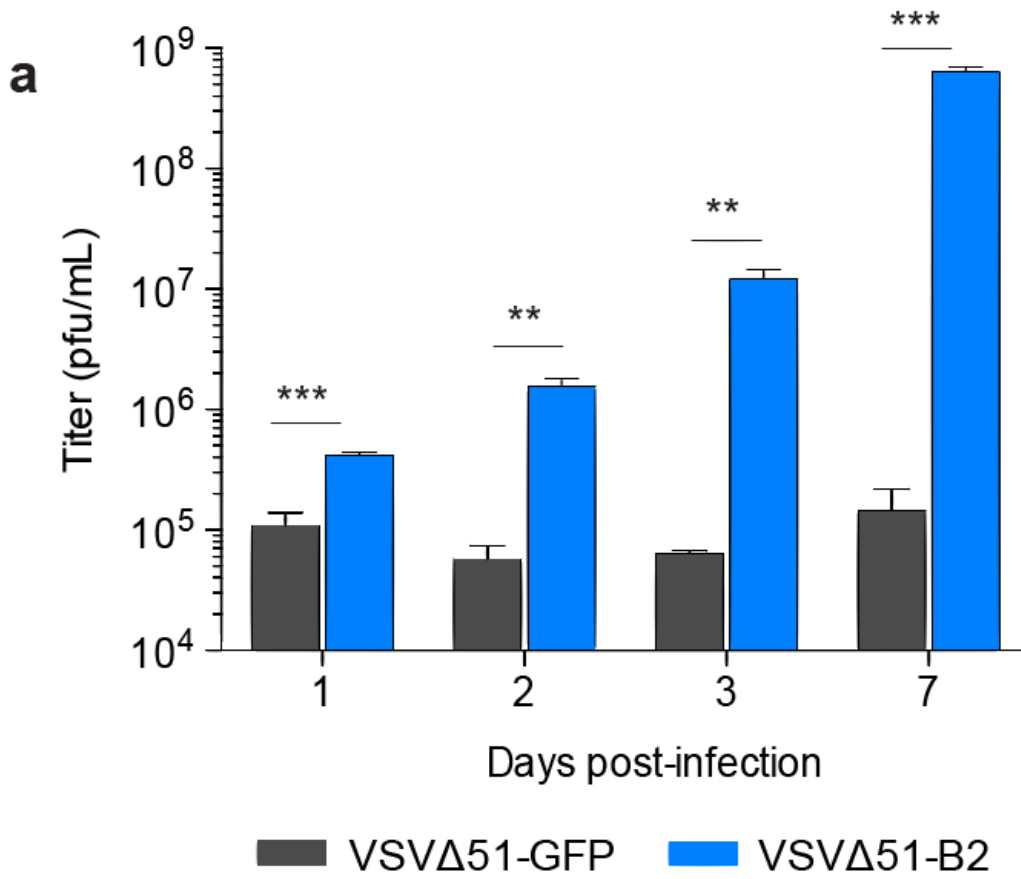


**Figure 3.4 B2 is functional in insect cells when expressed by VSV $\Delta$ 51** (A) Viral titers recovered from S2 Drosophila cells infected at an MOI of 10 with either VSV $\Delta$ 51-GFP or VSV $\Delta$ 51-B2. (B) Western blot analysis for VSV proteins and tubulin from VSV $\Delta$ 51-GFP or VSV $\Delta$ 51-B2-infected S2 Drosophila cell lysates 48 hpi. NS:  $P > 0.1$ , \* $P < 0.1$ , \*\* $P < 0.01$ , \*\*\* $P < 0.001$  (unpaired one-tailed T-test). Only significantly different pairs are indicated on the figure.

### **3.3 B2 expression improves VSV $\Delta$ 51 cytotoxicity in a panel of human cancer cell lines**

The previous data demonstrates the production of a functional B2 in insect cells, but the impact of virally-encoded B2 on mammalian tumor cells remained to be assessed. To determine if VSV $\Delta$ 51-B2 could kill tumor cells more efficiently compared to the parental virus, we screened a panel of 38 human cancer cell lines of various types. The cells were infected at a multiplicity of infection (MOI) of 1 and cell viability was assessed. Impressively, the B2-expressing virus showed enhanced killing in over 85% of the cell lines tested (Fig 3.5A). We repeated our screen using an additional virus variant encoding Vaccinia virus VP55, a different VSR, and found once again that cell killing was enhanced by the presence of the VSR (Fig 3.5B). Remarkably, this enhancement in virus-mediated killing was similar when comparing B2 to VP55 in all cell lines tested. To confirm the expected production of higher viral titers by the B2-expressing virus, we performed qPCRs for viral genomes in infected tumor cell lines and were able to detect higher levels of VSV genomes with VSV $\Delta$ 51-B2 infection compared to VSV $\Delta$ 51-GFP, specifically in cell lines we determined were sensitive to VSV $\Delta$ 51-B2 through our initial screen (Fig 3.6A). Furthermore, to ensure that B2 expression did not enhance virus replication in healthy cells, we infected GM38 fibroblasts with VSV $\Delta$ 51-B2 or VSV $\Delta$ 51-GFP and found that VSV $\Delta$ 51-B2 infection did not significantly increase viral cytotoxicity at an MOI of 1 (Fig 3.6B). Consistent with the qPCR data, growth curves performed on selected tumor cell lines showed enhanced replication of the B2 virus at the various time point tested (Fig 3.7).

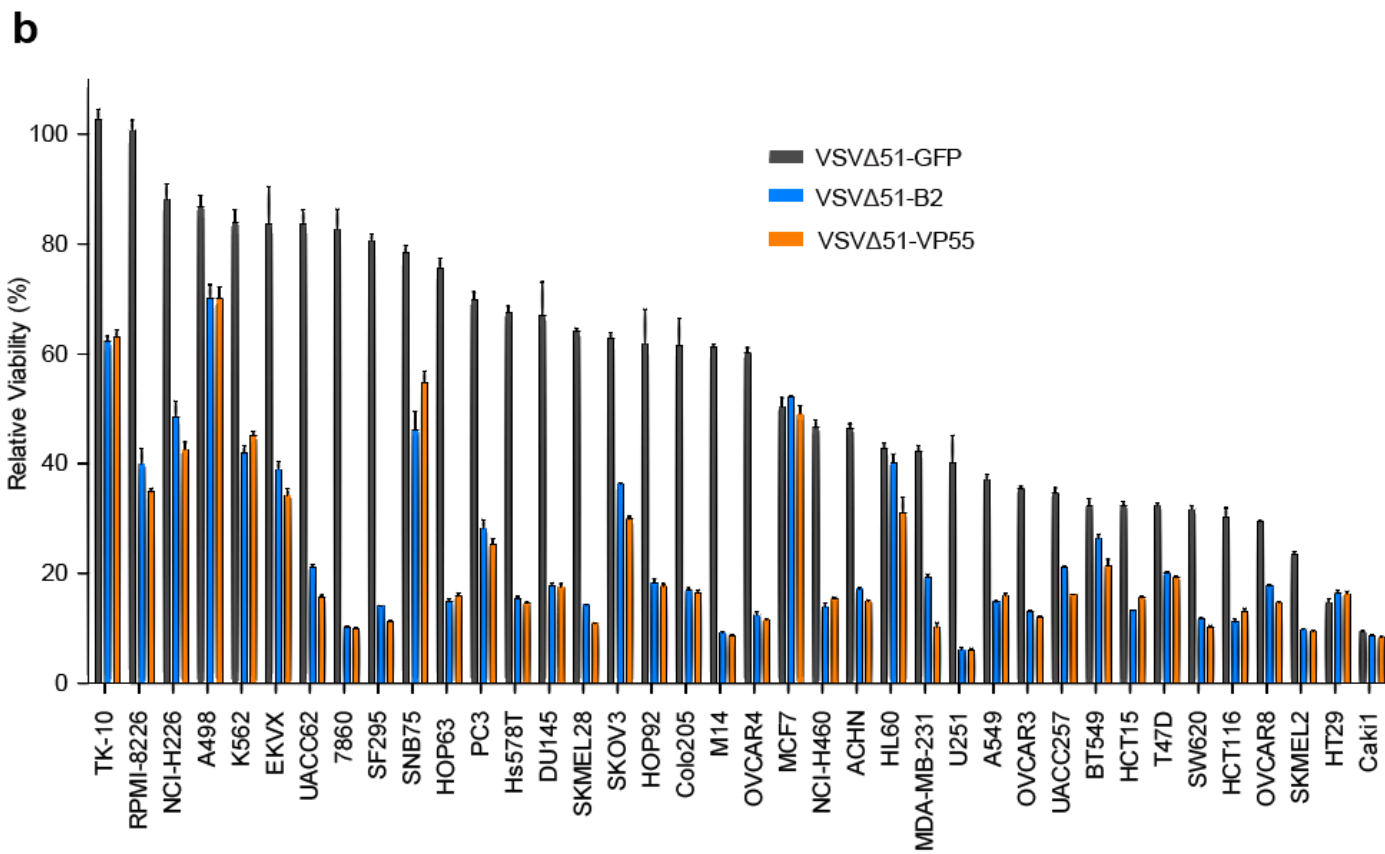
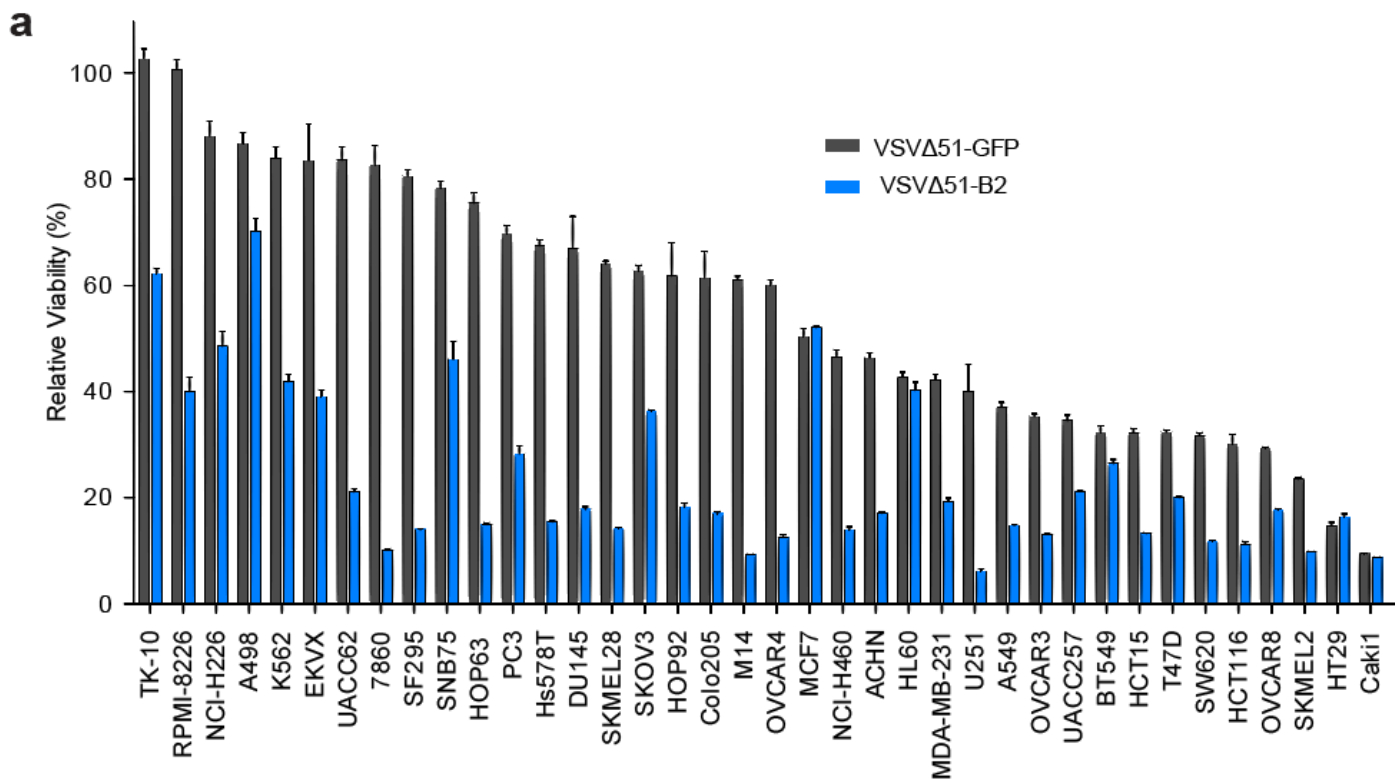


**Figure 3.5 VSV $\Delta$ 51-mediated expression of B2 enhances cytotoxicity in tumor cell lines.** (A) Relative metabolic activity of 38 human cell lines infected with VSV $\Delta$ 51-GFP or VSV $\Delta$ 51-B2 or additionally VSV $\Delta$ 51-VP55 (B) for 48h at an MOI of 1. The results are expressed as a percentage of the signal obtained compared to mock treatment.

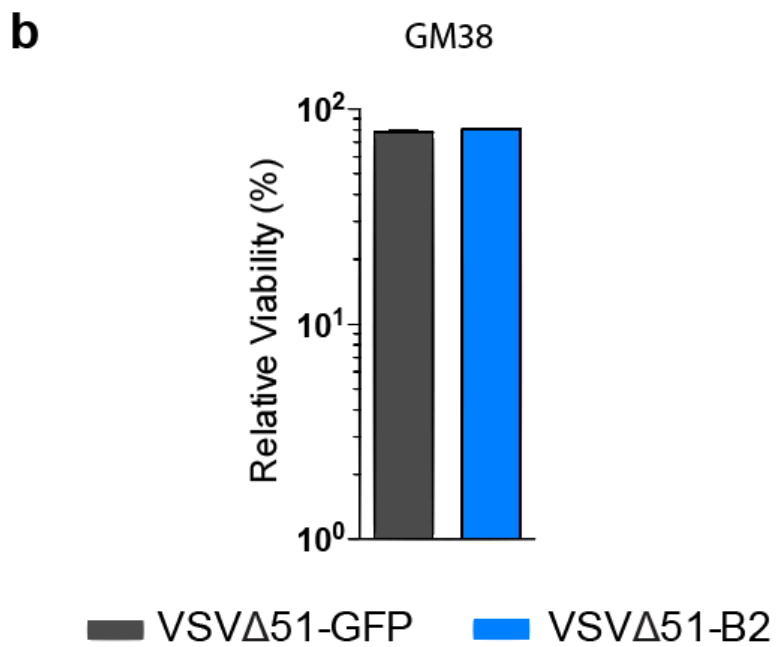
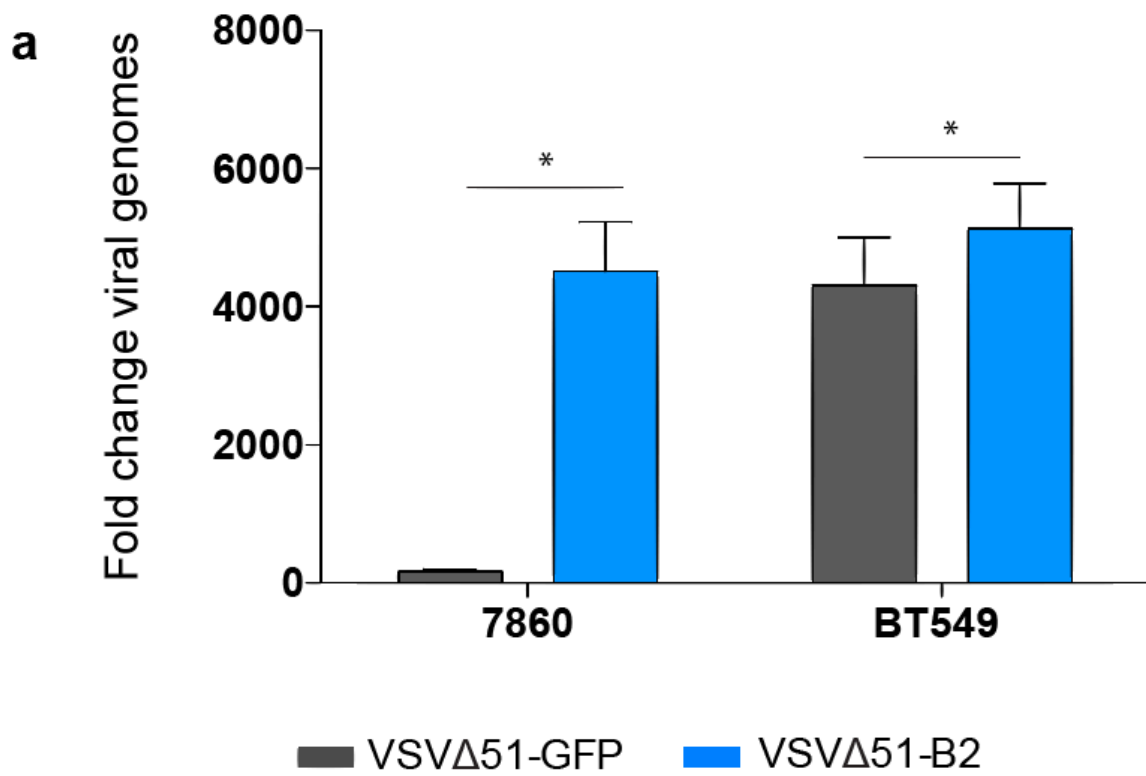


**Figure 3.6 VSV $\Delta$ 51-B2 enhances improves viral replication in cancer cells but not healthy cells.** (A) Fold change in VSV genomes, expressed relative to input levels. RNA for qPCRs was harvested from infected 7860 and BT549 cells at an MOI of 1 for 24h. (B) Relative metabolic activity of GM38 fibroblasts infected with VSV $\Delta$ 51-GFP or VSV $\Delta$ 51-B2 for 48h at an MOI of 1. The results are expressed as a percentage of the signal obtained compared to mock treatment. NS:  $P > 0.1$ , \* $P < 0.1$ , \*\* $P < 0.01$ , \*\*\* $P < 0.001$  (unpaired one-tailed T-test). Only significantly different pairs are indicated on the figure.

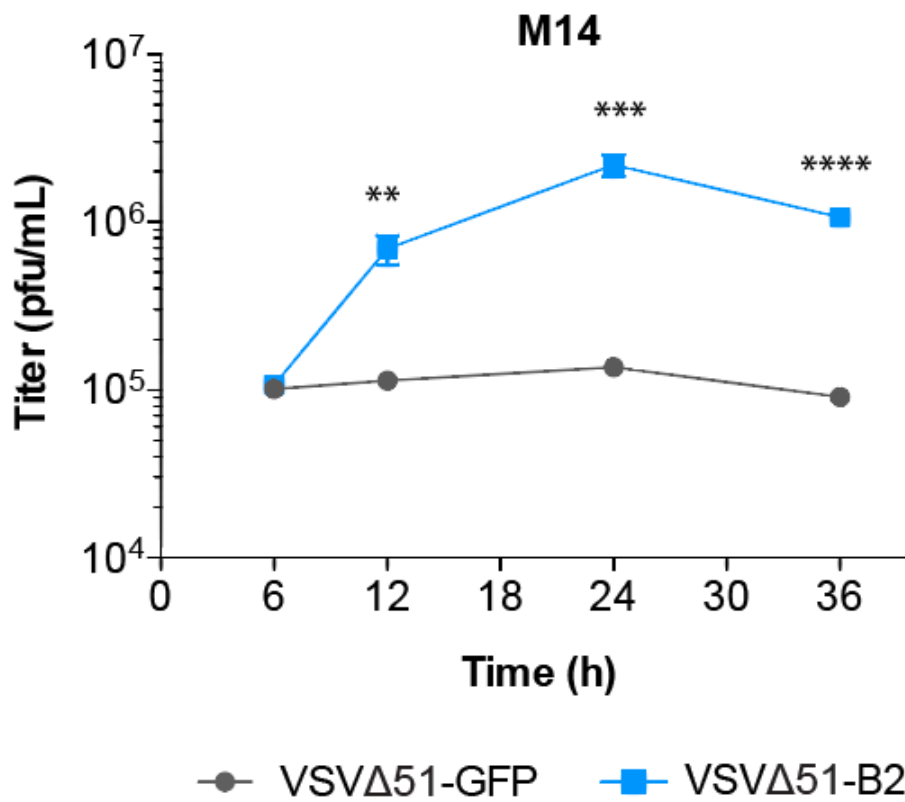
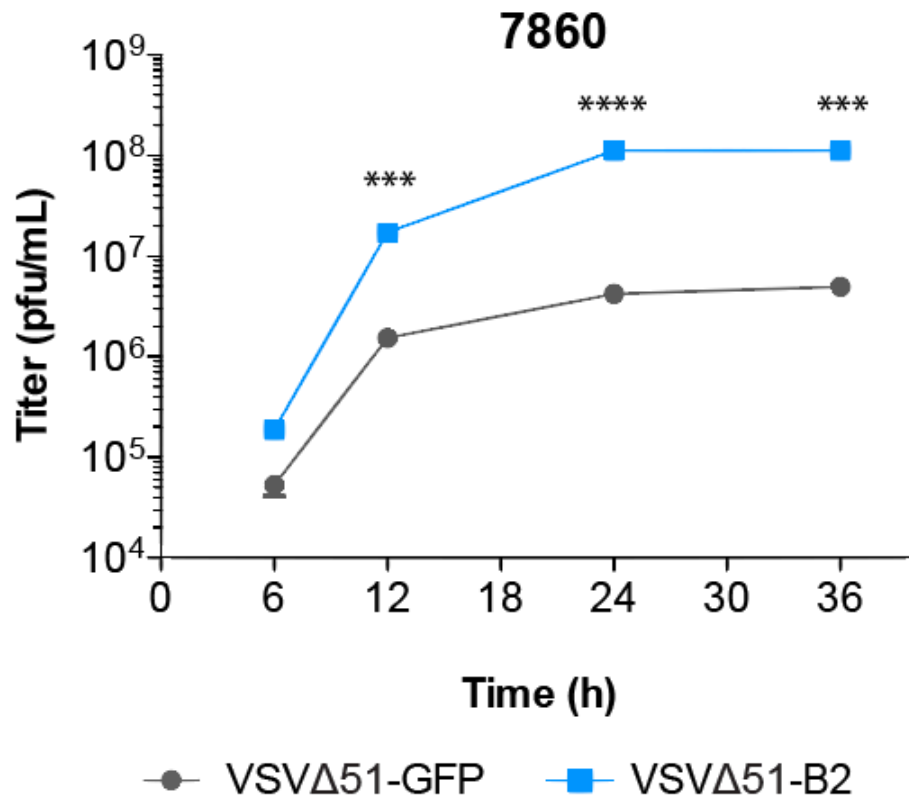


**Figure 3.7 Growth kinetics of VSV $\Delta$ 51-B2 in resistant cancer cell lines.** Time-course of viral titers from 7860 and M14 cell lines infected with VSV $\Delta$ 51-GFP or VSV $\Delta$ 51-B2 at an MOI of 3. NS: P>0.1, \*P<0.1, \*\*P<0.01, \*\*\*P<0.001 (unpaired one-tailed T-test). Only significantly different pairs are indicated on the figure.

### 3.4 VSV $\Delta$ 51-B2 alters microRNA levels and prevents VSV genome cleavage in cancer cells

It is well established that B2 blocks processing of small RNAs by Dicer in insect cells<sup>63,66</sup>. Given that B2 improves VSV $\Delta$ 51 production by mammalian tumor cells, we decided to investigate if microRNA levels were affected by VSV $\Delta$ 51-B2. To do so, we performed quantitative PCR (qPCR) for a panel of miRNAs from infected 7860s. For 6 out of the 7 miRNAs tested, the levels measured in VSV $\Delta$ 51-B2 infected samples were significantly lower compared to VSV $\Delta$ 51-GFP samples, therefore suggesting inhibition of small RNA processing (Fig 3.8). Furthermore, we compared the size distributions of small RNA reads to look for potential differences in RNA processing from VSV $\Delta$ 51-B2 and VSV $\Delta$ 51-GFP infected cancer cells. To do so, we performed deep sequencing for samples from a selection of infected cell lines and looked for the presence of a peak at approximately 22 to 23 nucleotides, the size of Dicer processed small RNAs (Fig 3.9). We were able to detect a peak corresponding to Dicer-cleaved products in the six cell lines tested. This peak was reduced in VSV $\Delta$ 51-B2 conditions in most cell lines compared to VSV $\Delta$ 51 as would be predicted given B2-mediated inhibition of RNA cleavage. We then looked specifically for Dicer-processed viral genomes and observed 22-23 nucleotides-long reads mapping to the VSV genome (Fig 3.10). Interestingly, we once again observed a reduction in this peak in the VSV $\Delta$ 51-B2 infected samples, suggesting that B2 may also prevent viral genome cleavage. Notably, this prevention in VSV genome cleavage was especially evident in the cell lines where no reduction was observed in the total RNA reads, unmapped to VSV (MCF7 and HCT116) (Fig 3.9). Taken together, these data demonstrate that VSV $\Delta$ 51-B2 inhibits direct cleavage of the viral genome as well as host RNA processing pathways.

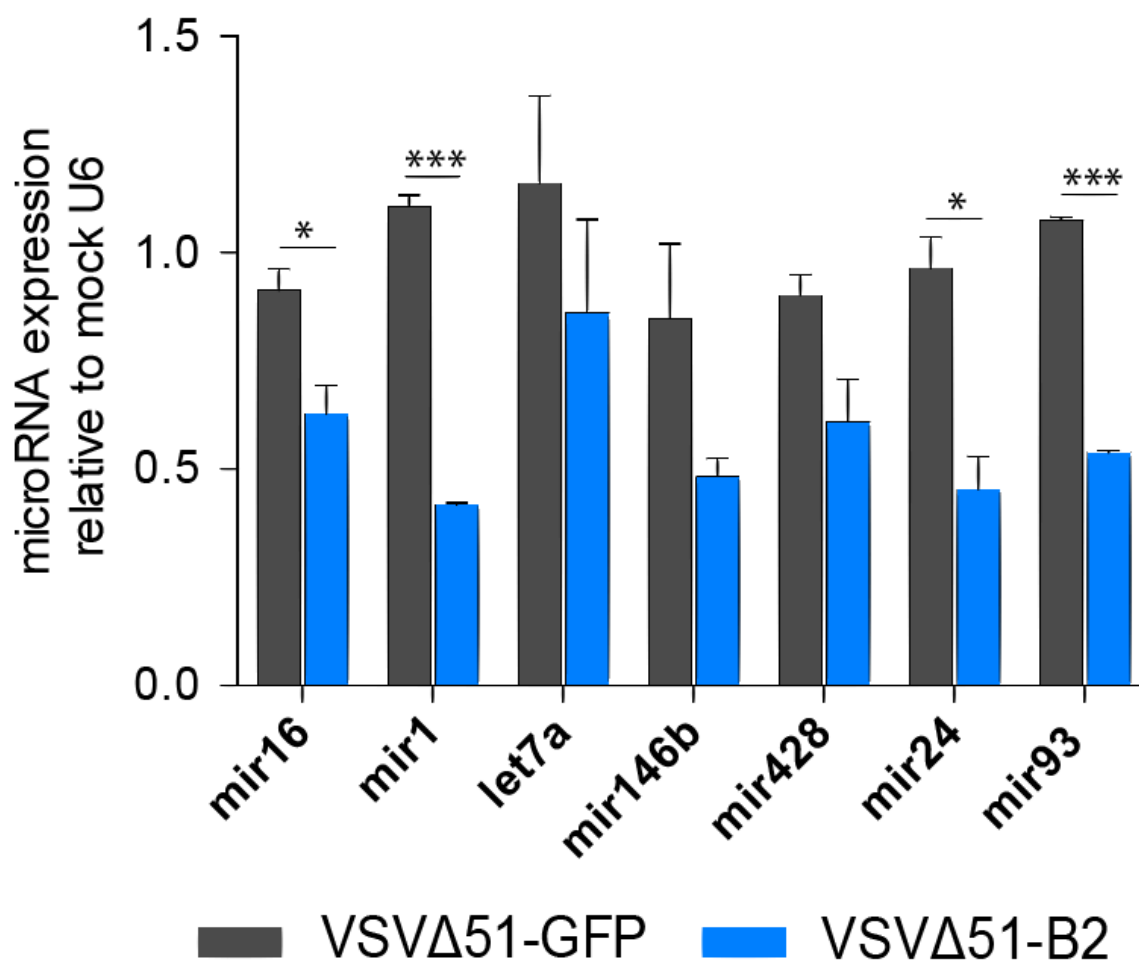


**Figure 3.8 VSV $\Delta$ 51-B2 alters microRNA levels in 7860s.** MicroRNA levels from 7860 cells infected with VSV $\Delta$ 51-GFP or VSV $\Delta$ 51-B2 for 18h as determined by qPCR. The results were normalized to mock uninfected levels as explained in the material and methods section. NS:  $P > 0.1$ , \* $P < 0.1$ , \*\* $P < 0.01$ , \*\*\* $P < 0.001$  (unpaired one-tailed T-test). Only significantly different pairs are indicated on the figure.

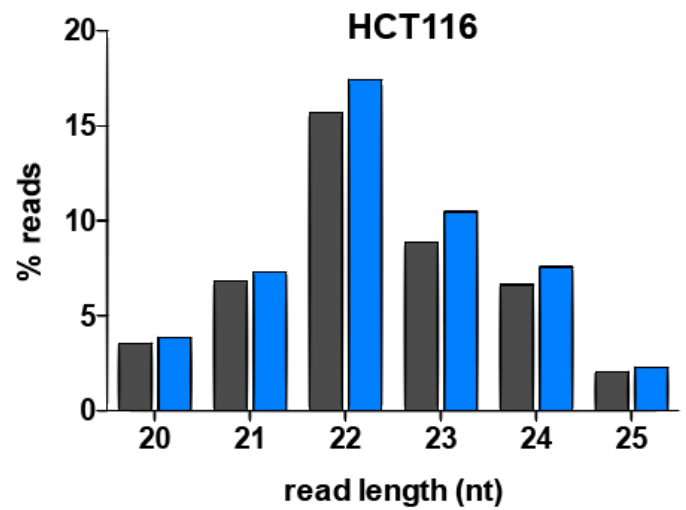
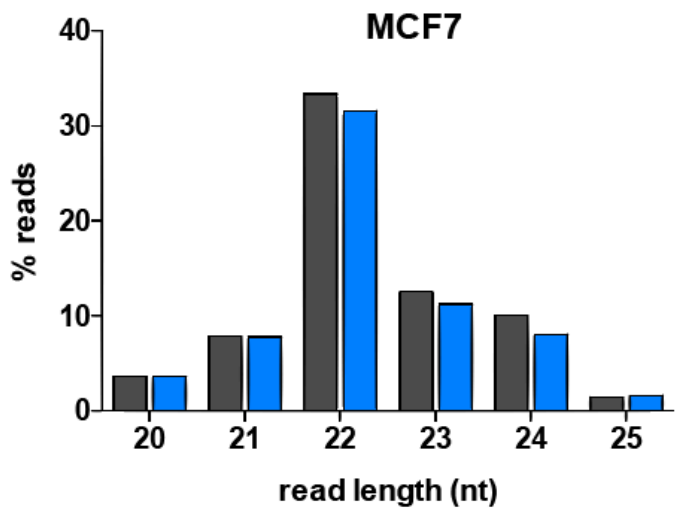
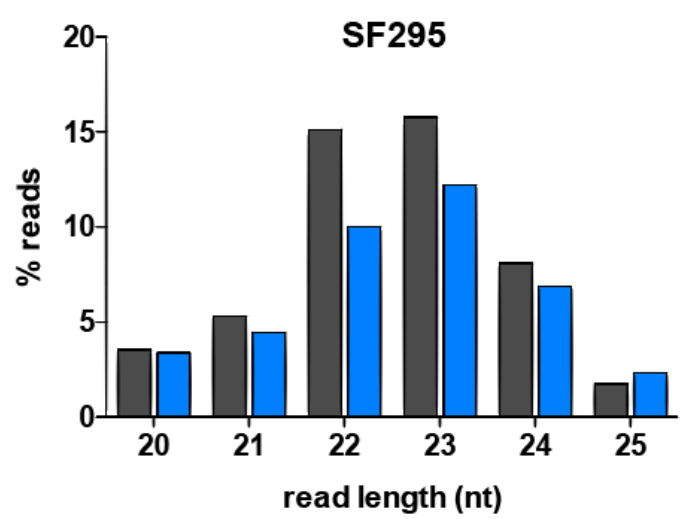
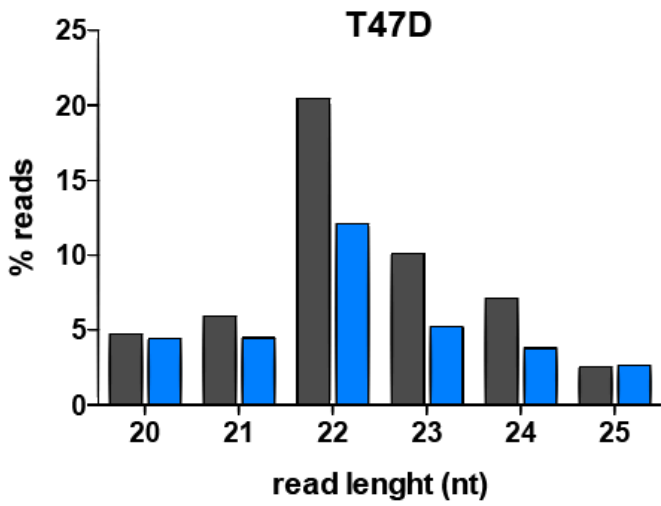
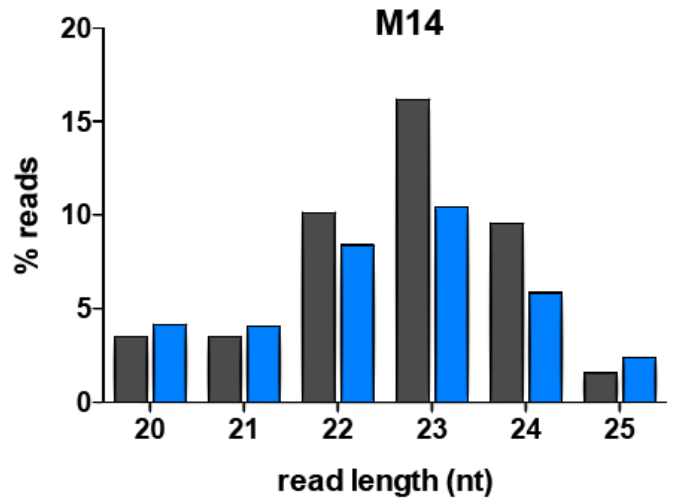
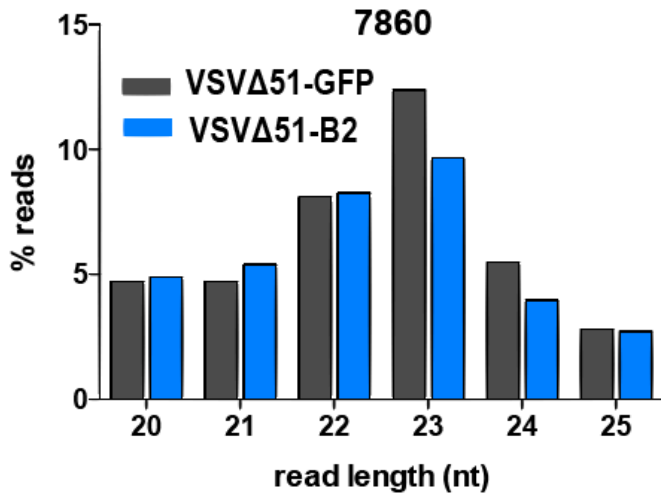


**Figure 3.9 VSV $\Delta$ 51-B2 alters RNA processing in various cancer cell lines.** Read length distribution of total small RNAs, including host-derived RNAs, from tumor cells infected with VSV $\Delta$ 51-GFP or VSV $\Delta$ 51-B2 at an MOI of 0.1 for 18h as determined by deep-sequencing.

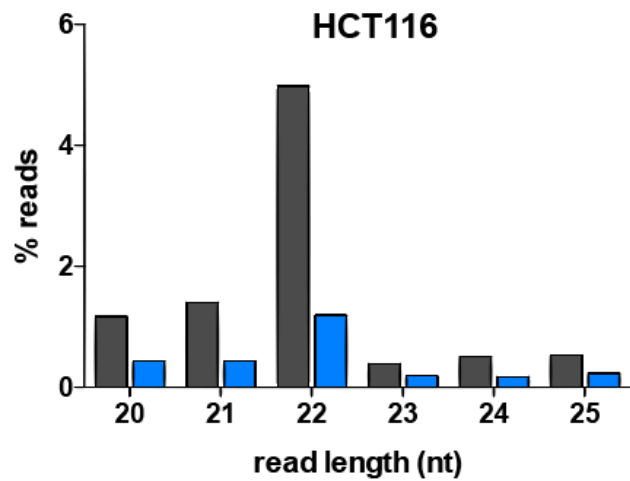
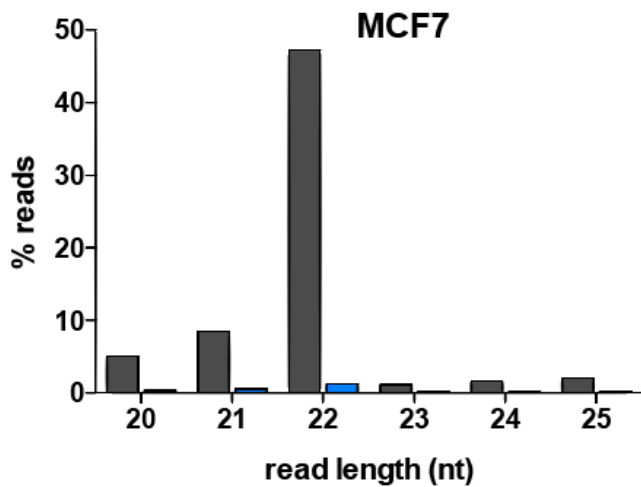
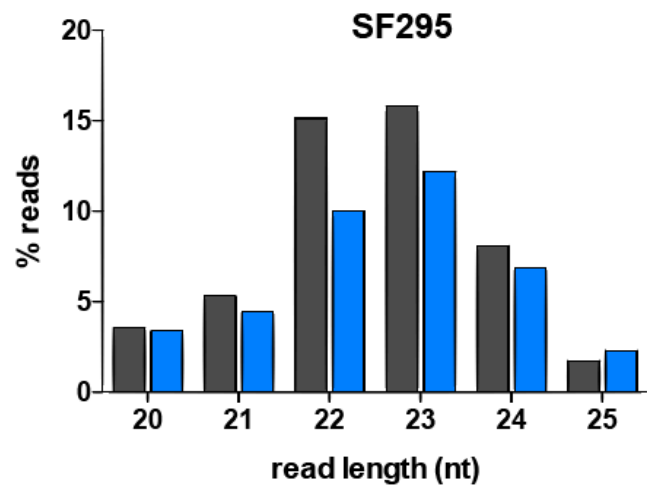
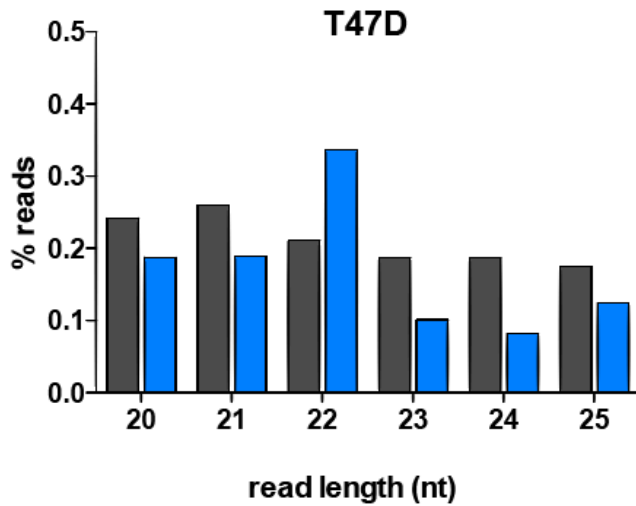
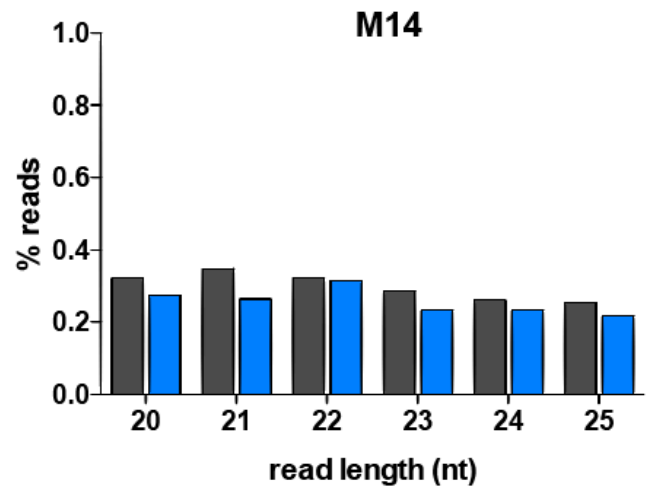
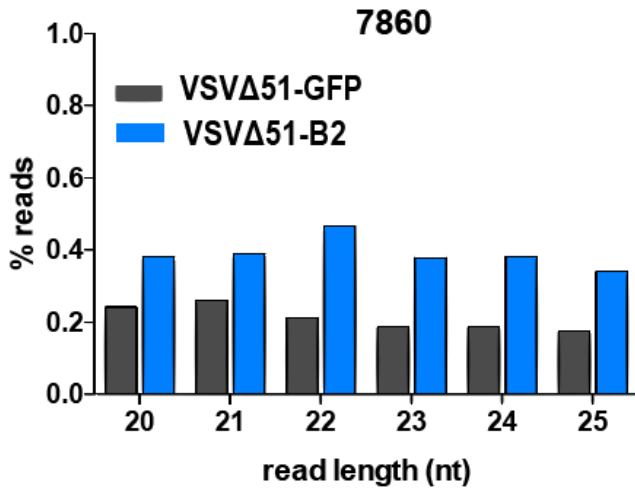


**Figure 3.10 VSV $\Delta$ 51-B2 inhibits viral genome cleavage in certain cancer cell lines.** Read length distribution of small RNAs mapping to the VSV genome from tumor cells infected with VSV $\Delta$ 51-GFP or VSV $\Delta$ 51-B2 at an MOI of 0.1 for 18h as determined by deep-sequencing.

### 3.5 VSV $\Delta$ 51-B2 and the Type I IFN response

In an attempt to characterize the effect of B2 expression on mammalian tumor cells, we performed a microarray analysis on samples from M14 cells infected with either VSV $\Delta$ 51-GFP or VSV $\Delta$ 51-B2. Our results show the increased induction of a number of genes related to the IFN response by VSV $\Delta$ 51-B2 compared to VSV $\Delta$ 51-GFP at the RNA level (Fig 3.11). We first confirmed the production of IFN $\beta$  by qPCR after infection of 7860 cells (Fig 3.12A). Consistent with our microarray results, we observed a significant increase by ELISA in IFN $\beta$  secretion in VSV $\Delta$ 51-B2 infected 7860 cells relative to VSV $\Delta$ 51-GFP (Fig 3.12B). We then performed qPCR for the genes MXA and OAS1, which are downstream of IFN $\beta$  and observed that despite the increase in IFN $\beta$  production with VSV $\Delta$ 51-B2, there is not as robust induction of these genes by the two viruses in infected 7860s (Fig 3.12C).

To determine the potential interplay between the IFN pathway and B2, we pre-treated M14 and 7860 cells with IFN followed by VSV $\Delta$ 51-B2 infection. We found that both M14 and 7860s could be protected by IFN pre-treatment as VSV $\Delta$ 51-GFP infection led to a reduction in cell killing in the presence of IFN (Fig 13A). Furthermore, IFN pre-treatment before VSV $\Delta$ 51-B2 infection appeared to partially protects the cells against VSV $\Delta$ 51-B2 (Fig 3.13A).

Lastly, we investigated if the production of VSV $\Delta$ 51-B2 could be even further enhanced by directly blocking IFN. We have previously described that B18R, an IFN scavenger expressed by Vaccinia virus, had the capacity to enhance VSV $\Delta$ 51 production<sup>88</sup>. In order to block the antiviral IFN that would be produced in response to VSV $\Delta$ 51 infection, we generated conditioned-media from vaccinia virus-infected cells and pre-treated tumor cells with this conditioned media. As usual, we found the viral titers to be significantly higher for VSV $\Delta$ 51-B2 with control media compared to VSV $\Delta$ 51-GFP (Fig 3.13B). VSV $\Delta$ 51-B2 titers with vaccinia virus conditioned-

media were only modestly higher from VSV $\Delta$ 51-GFP titers, which implies that B2 expression alone enhances viral titers and does not appear to be further increased by blocking the IFN response.

0 2 4 6 8

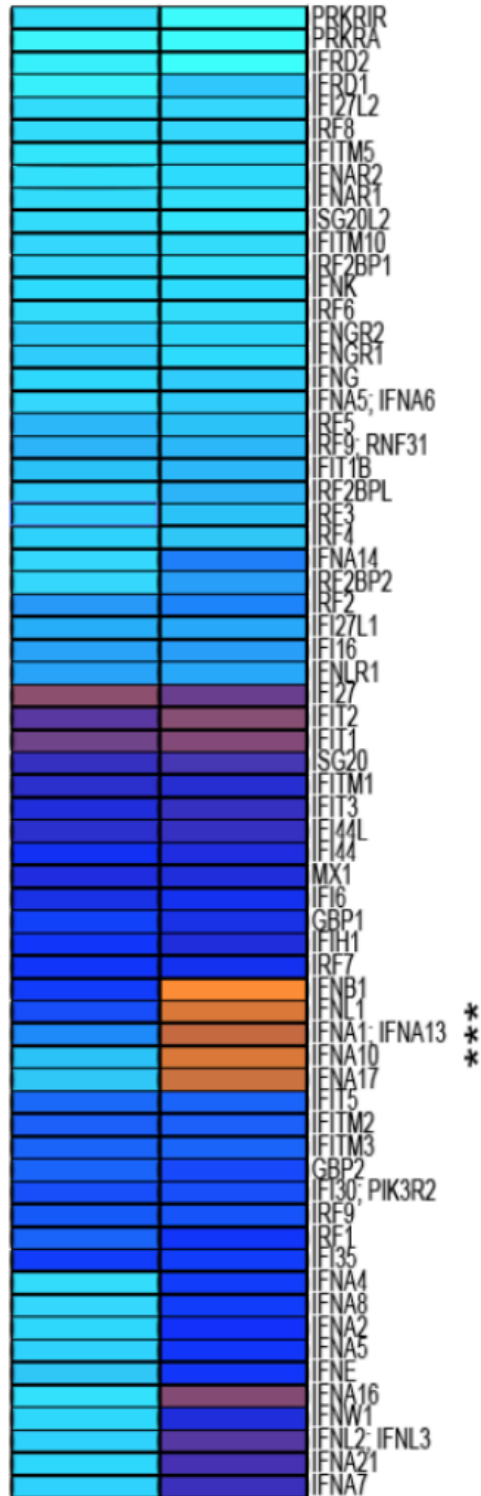


**Figure 3.11 VSV $\Delta$ 51-B2 infection upregulates interferon expression.** Microarray analysis of M14 cells infected with VSV $\Delta$ 51-GFP or VSV $\Delta$ 51-B2 at an MOI of 0.1 for 18h.

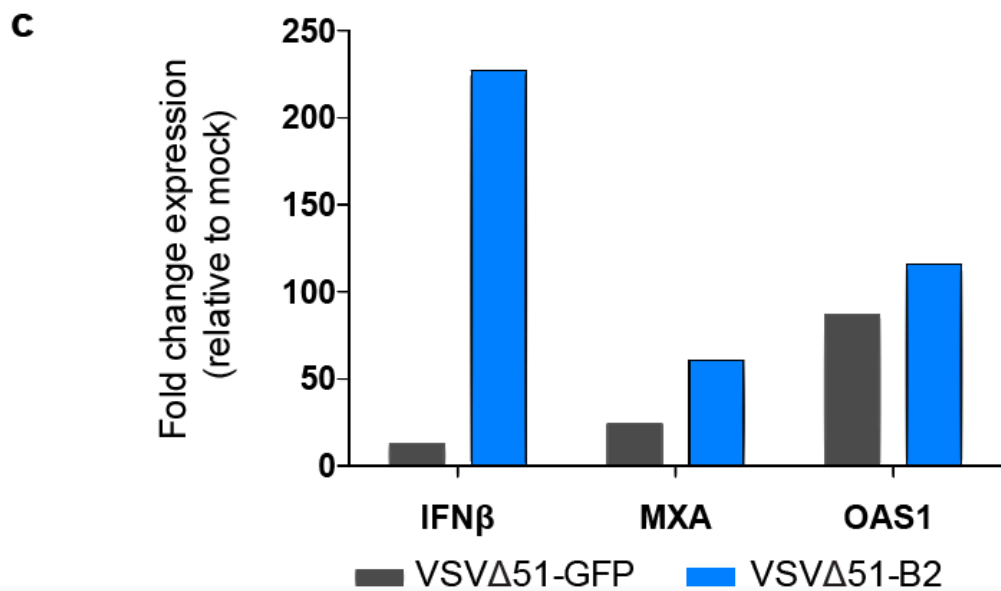
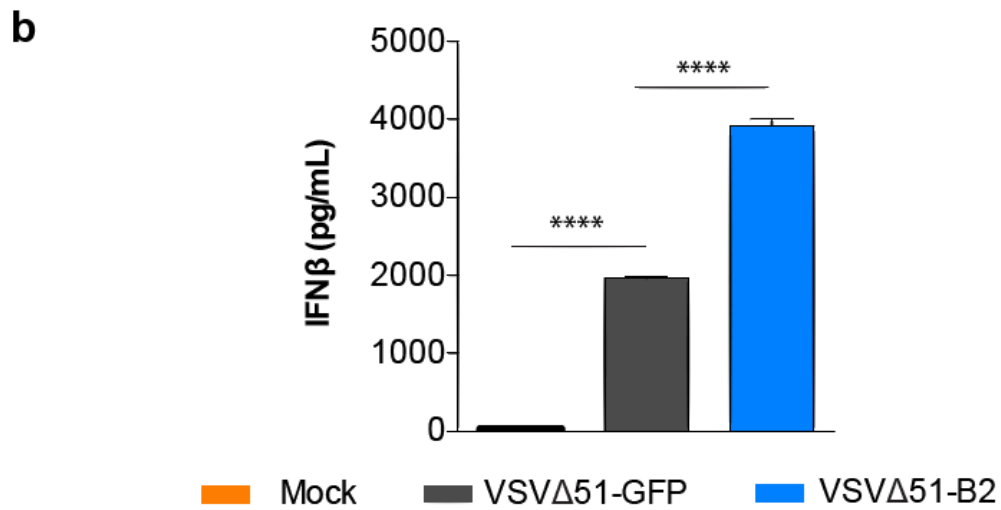
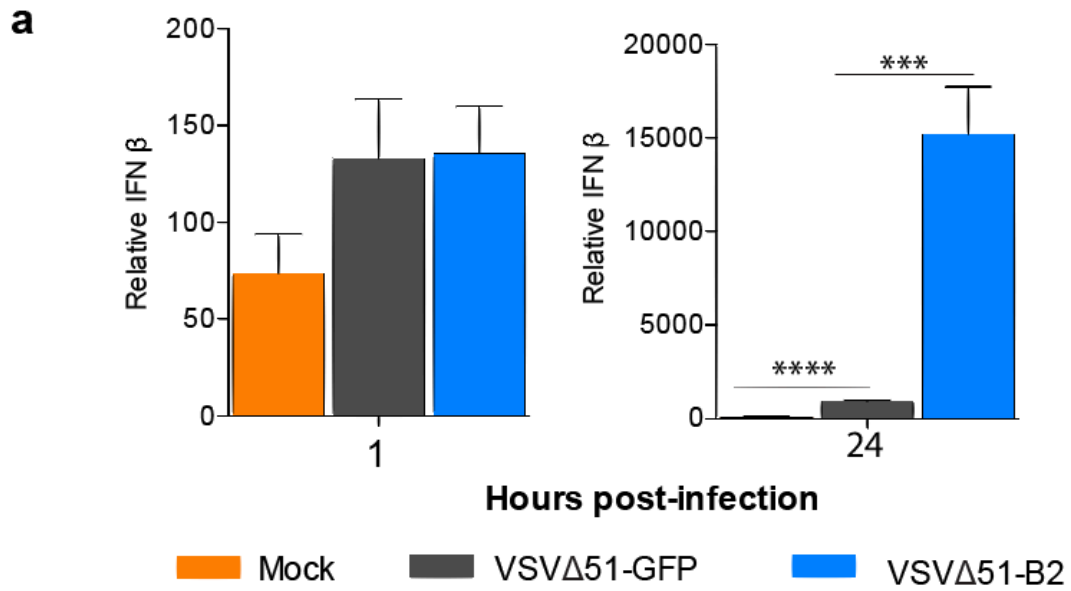
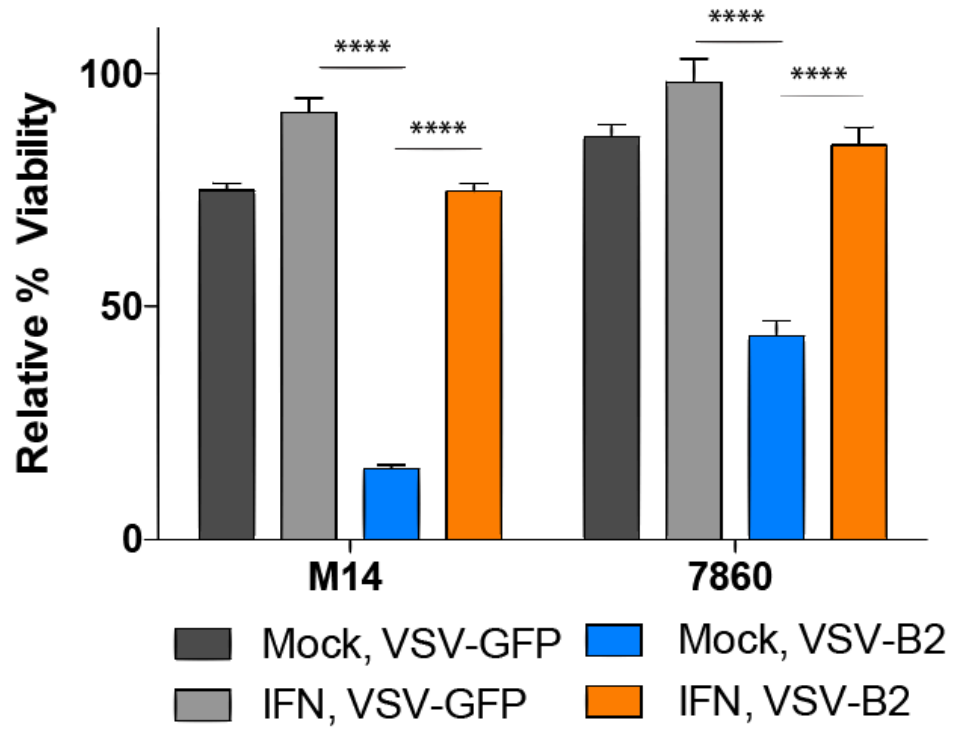


**Figure 3.12 The effects of VSV $\Delta$ 51-B2 on modulating the interferon response.** (A) qPCR analysis of IFN $\beta$  expression of 7860 cells infected for various times. IFN $\beta$  levels were normalized to GAPDH levels within each sample. (B) ELISA for IFN $\beta$  from supernatants of 7860 cells infected with VSV $\Delta$ 51-GFP or VSV $\Delta$ 51-B2 at an MOI of 0.1 for 24h. (C) Fold change relative to mock in levels of IFN $\beta$ , MXA and OAS1 in 7860 cells infected with VSV $\Delta$ 51-GFP or VSV $\Delta$ 51-B2 at an MOI of 0.1 for 24h. NS: P>0.1, \*P<0.1, \*\*P<0.01, \*\*\*P<0.001 (unpaired one-tailed T-test). Only significantly different pairs are indicated on the figure.

**a**



**b**

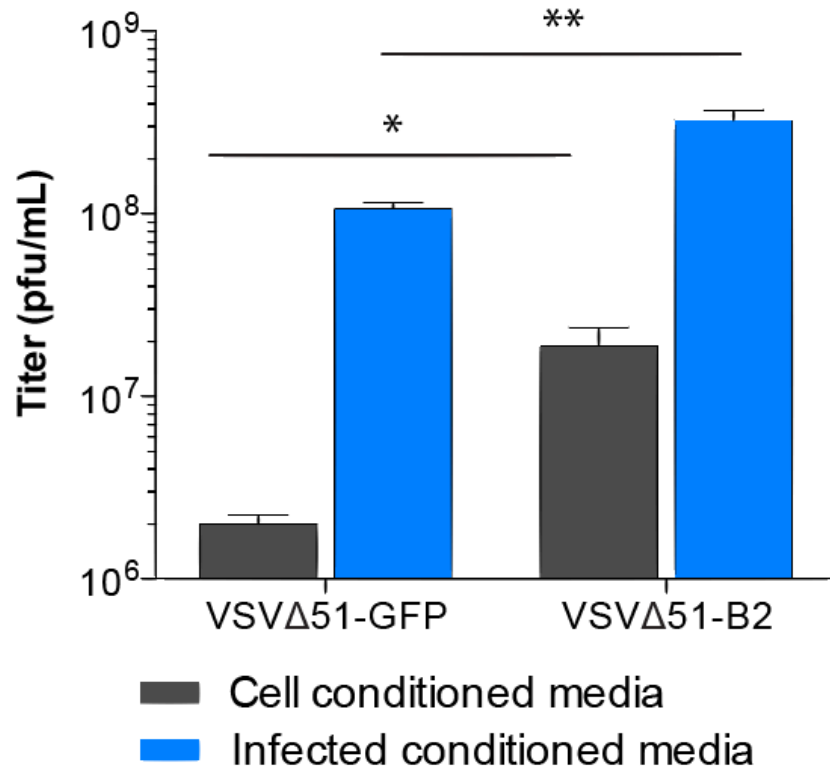
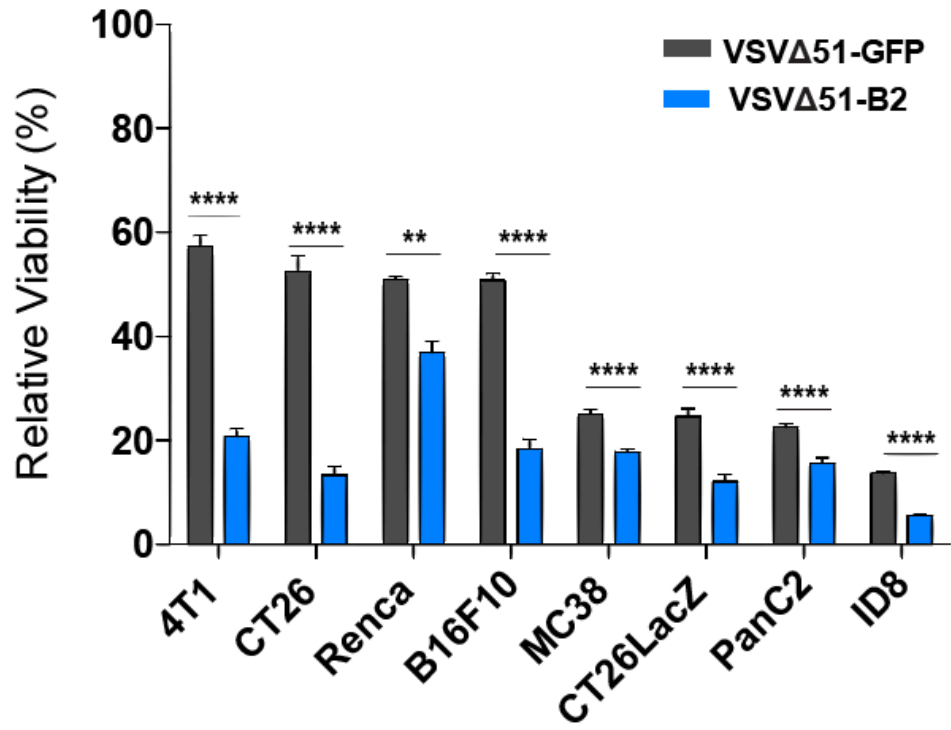


**Figure 3.13 The effects of interferon pre-treatment or blocking on VSVΔ51-B2 infection.** (A) Relative metabolic activity of M14 or 7860 cells infected with VSVΔ51-GFP or VSVΔ51-B2 for 48h at an MOI of 1, with or without 4h pre-treatment with 50 IU/mL universal interferon. The results are expressed as a percentage of the signal obtained compared to mock treatment. (B) Virus outputs of VSVΔ51-GFP and VSVΔ51-B2 obtained from 7860 cells pre-treated with Vaccinia virus conditioned-media. Virus-cleared supernatants from Hela cells that were infected with Vaccinia virus at an MOI of 1 for 48h or left uninfected were transferred onto 7860 cells prior to infection with VSVΔ51-GFP or VSVΔ51-B2 for 48h. NS:  $P > 0.1$ ,  $*P < 0.1$ ,  $**P < 0.01$ ,  $***P < 0.001$  (unpaired one-tailed T-test). Only significantly different pairs are indicated on the figure.

### **3.6 Virus-mediated B2 expression enhances tumour-specific replication and increases cytokine production**

To establish an *in vivo* model, we began by screening a number of murine cell lines *in vitro* with VSV $\Delta$ 51-B2 to choose a cell line for which VSV $\Delta$ 51-B2 shows enhanced cytotoxicity (Fig 3.14A). We found that, as observed using the human cell lines, the murine tumor cells were more efficiently killed by the B2 virus. We proceeded to use one of these cell lines *in vivo*; the Renca renal carcinoma cell line, which is syngeneic to Balb/c mice. In addition, we used the human M14 melanoma cell line that can be grown as xenografts in nude mice. For both tumor models, VSV $\Delta$ 51-B2 titers from subcutaneous tumours harvested 24 h post-intratumoral injection were significantly higher compared to VSV $\Delta$ 51-GFP (Fig 3.14B). Interestingly and consistent to what we observed *in vitro* in our microarray analysis, the IFN $\gamma$ , TNF $\alpha$  and CCL2 concentrations from the serum of the VSV $\Delta$ 51-B2 treated mice were higher compared to VSV $\Delta$ 51-GFP treated mice (Fig 3.15). Also consistent to the *in vitro* data demonstrating that the B2-encoding virus does not replicate better compared to the parental virus in the GM38 fibroblast cell lines, a biodistribution analysis following intravenous administration revealed unchanged distribution of VSV $\Delta$ 51 and VSV $\Delta$ 51-B2 in various organs (Fig 3.16).

**a**



**b**

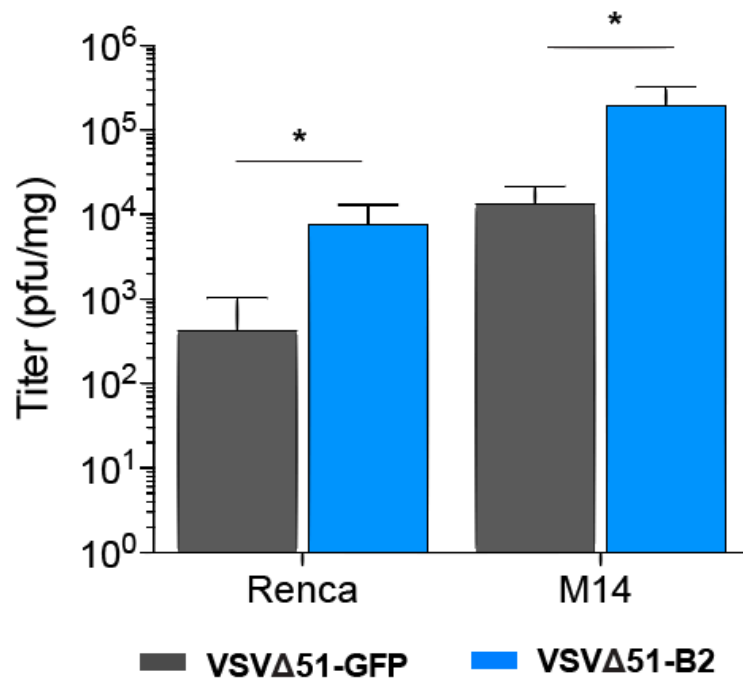


**Figure 3.14 VSV $\Delta$ 51-B2 enhances replication within murine cell lines and tumour models.** (A) Relative metabolic activity of murine cell lines infected with VSV $\Delta$ 51-GFP or VSV $\Delta$ 51-B2 for 48h at an MOI of 1. The results are expressed as a percentage of the signal obtained compared to mock treatment. (B) Viral titers obtained 24 hpi from subcutaneous M14 or Renca tumours. Virus was administered intratumourally at a dose of 1E9 pfu of VSV $\Delta$ 51-GFP or VSV $\Delta$ 51-B2. NS: P>0.1, \*P<0.1, \*\*P<0.01, \*\*\*P<0.001 (unpaired one-tailed T-test). Only significantly different pairs are indicated on the figure.

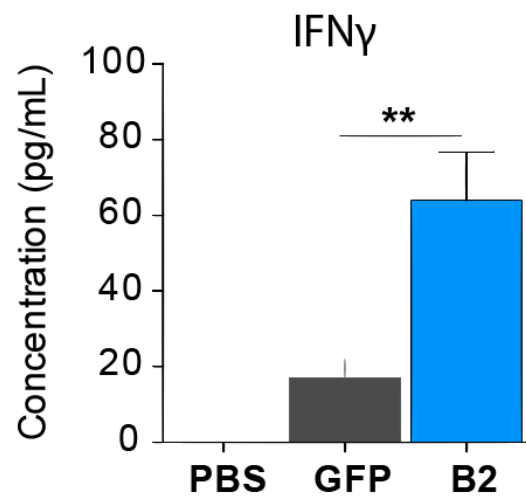
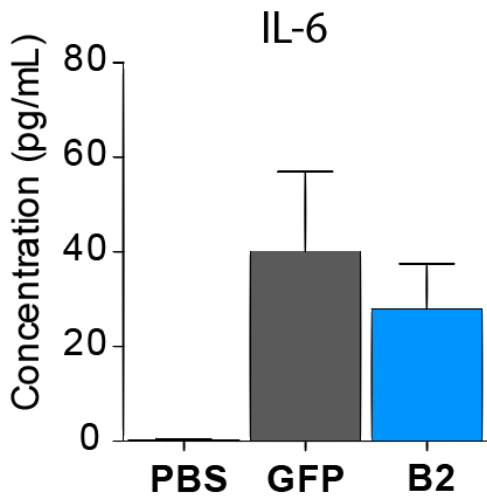
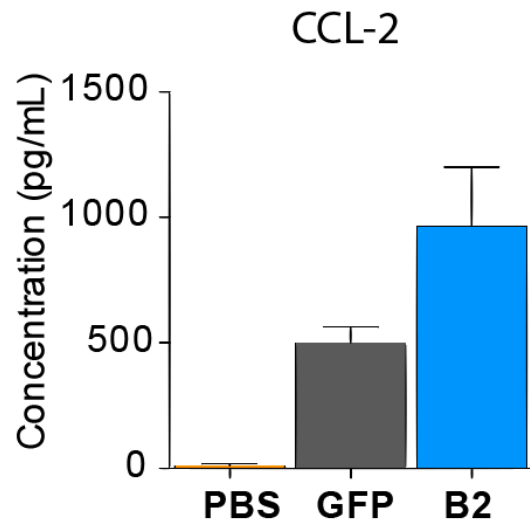
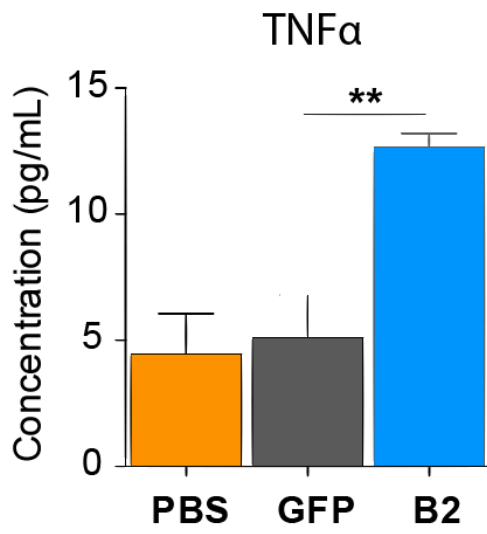


**Figure 3.15 VSV $\Delta$ 51-B2 treatment enhances serum cytokine levels in the Renca tumour model.** Serum levels of TNF $\alpha$ , CCL2, IL-6 and IFN $\gamma$  from Renca tumour-bearing C57BL/6 mice. Virus was administered intratumourally at a dose of 1E9 pfu of VSV $\Delta$ 51-GFP or VSV $\Delta$ 51-B2 and serum collected 24 hpi. NS: P>0.1, \*P<0.1, \*\*P<0.01, \*\*\*P<0.001 (unpaired one-tailed T-test). Only significantly different pairs are indicated on the figure.

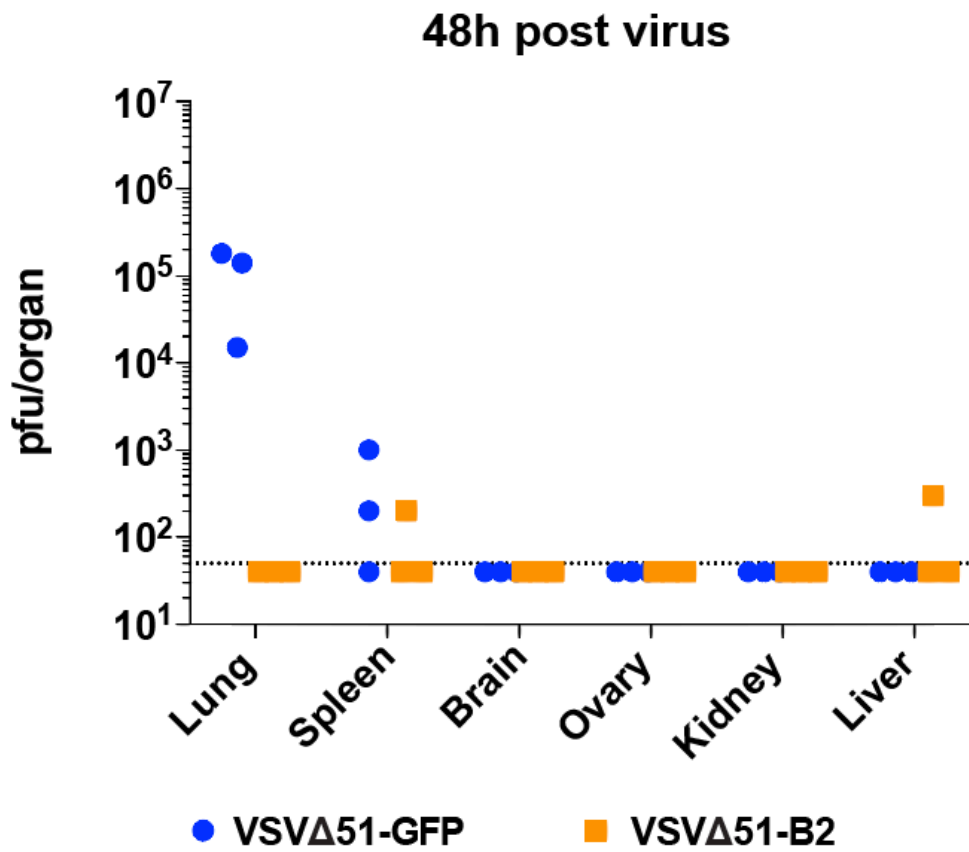
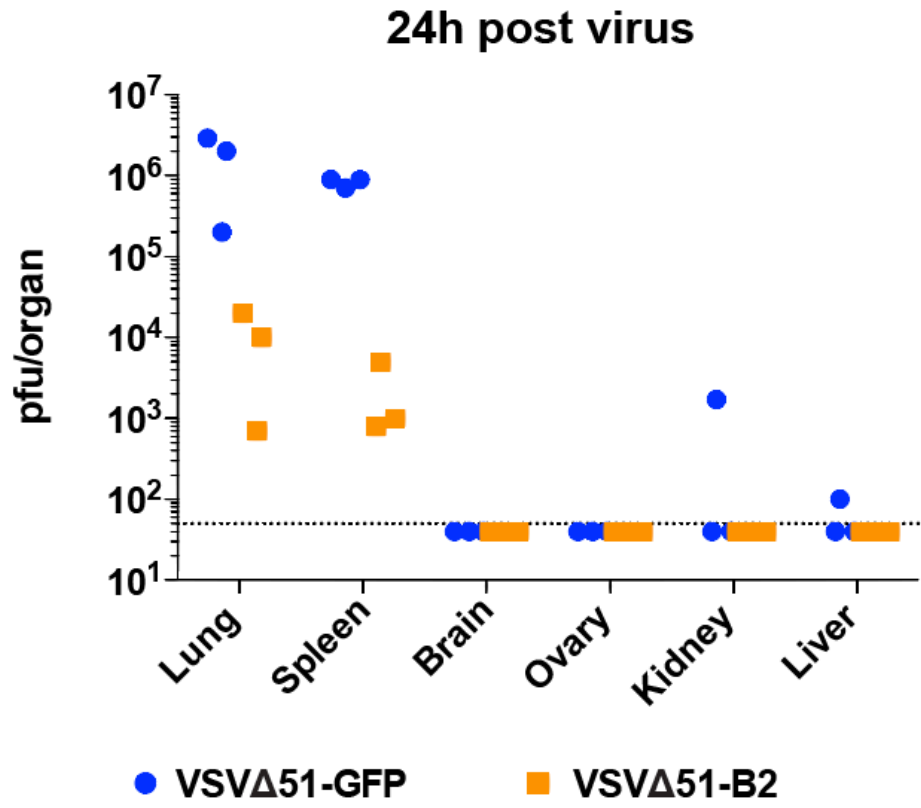


**Figure 3.16 Biodistribution of VSV $\Delta$ 51-B2 in tumour-bearing C57BL/6 mice.** Viral titers obtained 24 or 48 hpi from organs of tumour-bearing C57BL/6 mice. Virus was administered intravenously at a dose of 1E9 pfu of VSV $\Delta$ 51-GFP or VSV $\Delta$ 51-B2. For organs where virus was undetectable, the titer was considered to be the value of the limit of detection of titering for this assay (5E1 pfu/organ). NS: P>0.1, \*P<0.1, \*\*P<0.01, \*\*\*P<0.001 (unpaired one-tailed T-test).

## 4. Discussion

### 4.1 A novel role for antiviral RNAi in human cancers

The role of viral genome cleavage in controlling VSV infection has been extensively demonstrated in the context of insects and invertebrates but our data indicating that antiviral RNAi is functioning in cancer cells is completely novel and this is consistent with various reports. First, the fact that many mammalian viruses encode VSRs<sup>60</sup> supports the concept of a mammalian RNAi system and second, the demonstration that antiviral genome cleavage occurs in mammalian pluripotent cells<sup>78,79</sup>. Our initial objective was to determine whether anti-viral RNAi may also function in cancer cells. We were able to detect viral genome fragments peaking at 21-23 nt of length, corresponding to the size of dicer cleavage products, following infection with VSV $\Delta$ 51 in a number of human cancer cell lines (7860, M14, T47D, SF295, MCF7 and HCT116). This finding supports our hypothesis that viral genome cleavage is occurring in certain cancer cells (Fig 3.10) and to our knowledge, this is the first report of this phenomenon in cancer cells.

Given that B2 is known to inhibit viral genome cleavage, we investigated the possibility that it might directly inhibit this cleavage. As expected, infection with VSV $\Delta$ 51-B2 resulted in a decrease in the cleaved viral genome fragments observed in some cell lines (7860, M14, T47D and SF295) (Fig 3.10). It is important to consider that although the size distribution of RNA reads suggests dicer-dependent cleavage additional experiments and analysis of sequencing would further confirm this. An important analysis which should be done with the sequencing data is to determine the phase registry of the 22 nt reads which map to the VSV genome. This analysis would determine if positive and negative strand 22 nt reads form complimentary duplexes with 2 nt 3' overhangs, features which are indicative of dicer-mediated processing. Another example, RNA co-immunoprecipitation of Ago2 followed by deep sequencing of bound RNA could establish if

these viral RNA fragments are indeed loaded into RISC as would be expected for classical dicer-dependent RNAi processing. Also, our read-length distribution analysis could be repeated in dicer knock-down cell lines. The loss of the peak at 21-23 nt in these cells would confirm a role for the RNAi pathway and rule out non-specific degradation. Using these same dicer knock-down cells lines, it would be interesting to determine if VSV $\Delta$ 51-B2 still has enhanced efficacy and therefore provides benefits even in the absence of a fully functional dicer.

#### **4.2 The controversy on mammalian RNAi**

The concept of an antiviral RNAi system in mammalian cells remains a highly debated subject. The fact that the mammalian antiviral response is quite different depending on the differentiation state adds to the confusion. A large body of literature exists to support the notion that differentiated cells rely on the IFN response over RNAi to combat virus infection and this is well-established for epithelial cells, fibroblasts and lymphocytes<sup>15</sup>. In contrast, undifferentiated mammalian cells, including embryonic stem cells<sup>80</sup>, oocytes<sup>77,89</sup>, teratocarcinomas<sup>90</sup> and embryonic carcinoma cells<sup>91</sup>, have attenuated IFN-responses and activate an RNAi-like response upon viral infection. In addition to the above, it has been shown that inactivating the VSRs of certain viruses does not rescue viral growth in somatic cells. For example, the LaCrosse Bunyavirus (LACV) encodes a VSR known as NS which induces apoptosis as well as blocks RNAi in insect cells<sup>92</sup>. LACV encoding a non-functional NS has attenuated replication in IFN-competent MEFs but its replication is unaffected in the absence of type I IFN receptors<sup>92</sup>. This suggests that the function of NS in inhibiting the antiviral response is mainly through IFN and not only via inhibition of antiviral RNAi. This further emphasizes a key component of our hypothesis which is that cancer cells differ from somatic cells. We suggest that given their known defects in the IFN response, the antiviral defense of cancer cells may more closely resemble that of pluripotent cells

like stem cells that have deficient Type I IFN responses as well as reduced expression of PRRs such as OAS1, PKR, MDA5, TLR3<sup>80,93</sup>. Interestingly, a reduced expression of these components have also been observed in various cancers. For example, lower PKR expression has been observed in lung cancers. Also PKR expression positively correlates with the degree of differentiation and aggressiveness of breast and head and neck cancers<sup>94-96</sup>. Our detection of virus-derived siRNAs in certain cancer cell lines suggests RNAi can be triggered in response to pathogen-associated signals. Whether the status of the IFN response pathway within these cell lines is connected to the existence of an RNAi response warrants further investigation. A comparison of the IFN responsiveness of cell lines where RNAi is or is not observed could provide insights in the crosstalk between RNA- and protein-mediated antiviral pathways. One interesting aspect would be to determine whether dsRNA binding PRRs retain full functionality and signaling abilities. Perhaps, in healthy tissues, PRRs sequester dsRNA into the IFN pathway whereas their reduced levels in cancer would allow for the entry of dsRNA into an RNAi-like antiviral pathway. It would therefore be of interest to investigate if the expression of various PRRs is increased in cancer cell lines as well. Finally it is important to note that although initial reports of mammalian antiviral RNAi suggest that this pathway is only functional in IFN non-responsive cells, a recent publication has demonstrated that IFN-functional 293T cells produce abundant virus-derived siRNAs<sup>97</sup>. Also, the fact that the RISC complex component Ago2 is inhibited upon viral infection further supports a role for the RNAi pathway in the antiviral response of these cells.<sup>98</sup> Indeed, it has recently been shown that loss of function mutations of Ago2 enhances replication of Influenza A, Encaphalomyocarditis virus and VSV in differentiated mammalian somatic cells<sup>97</sup>. Given that a number of cancer cell lines in our screen still respond to IFN, both mechanisms could potentially be contributing simultaneously.

### **4.3 Enhanced cell killing of VSV $\Delta$ 51-B2 in human cancer cell lines**

In this study, we demonstrate that B2 expression is sufficient to enhance VSV $\Delta$ 51 cytotoxicity and replication (Fig 3.1B, 3.5, 3.6A, 3.7) in cancer cells. Indeed, our screen of a panel of human cancer cell lines demonstrated enhanced killing by VSV $\Delta$ 51-B2 in over 85% of the cell lines tested (Fig 3.5). Impressively, VSV $\Delta$ 51-B2 appeared to have no specificity for the cancer type or tissue of origin. It is important to note that two out of the four cell lines in which there was no difference in cytotoxicity between the two viruses were the most sensitive to viral infection (HT29 and Caki-1). This suggests that virus-mediated killing might already be maximized in these cells. An antiviral RNAi system may still function in these cells but could only be effective in certain conditions, such as within the tumor microenvironment where additional barriers to infection are present. The two other cell lines in which VSV $\Delta$ 51-B2 did not perform better than VSV $\Delta$ 51-GFP were the MCF7 and HL60 cell lines. Interestingly, we did observe direct viral genome cleavage in the MCF7 cell line and inhibition by VSV $\Delta$ 51-B2. It is possible that other virus-induced factors could contribute to limiting virus-mediated killing and function to control VSV infection. For example, limiting viral genome transcription or virus assembly or budding would also impair virus production. For instance, it could be that assembly of new virions is impaired or already maximal within this cell line and despite the improved viral replication with B2 expression, increased viral genome levels do not correspond with increased production of virus particles. Quantitative PCR for processed VSV transcripts versus the viral genome itself could begin to answer whether genome transcription is being altered within certain cell lines. Furthermore, the IFN responsiveness and production status of the MCF7 cell line could provide an additional explanation. If Type I IFN defects are minimal within this cell line it could be that IFN is the predominant pathway for controlling VSV infection and therefore control even the increased

levels of virus when B2 is present. Based on this theory, these cell lines should behave similarly to infected GM38 cells which is true for MCF7s. Interestingly, triggering the IFN response has been shown to inhibit RISC function in certain mammalian somatic cells and therefore perhaps cancers with less severe IFN defects could produce viral siRNAs however these would ultimately non-functional<sup>98</sup>. Finally, as our readout for cell viability is an indirect readout based on metabolic activity, it would be ideal to have screening data using a direct method for quantifying cell death such as through quantifying LDH or caspase levels or by using an annexin V-propidium iodide assay. In addition, cell killing is only one readout to monitor infection. There may be an observable difference to infection with VSV $\Delta$ 51-B2 in other assays such as in viral titers which does not necessarily correspond to a difference in cell killing.

#### **4.4 RNAi inhibition through the Vaccinia virus VSR, VP55, enhances VSV $\Delta$ 51 killing**

Interestingly, our results show that VSV variants encoding B2 or VP55, two VSRs that impair the RNAi response by different mechanisms, show the same improvement in killing for all cell lines tested (Fig 3.5B). The mechanism of B2 involves binding of small RNA fragments to prevent processing by Dicer as well as loading into RISC<sup>63,66</sup>. On the other hand, VP55 polyadenylates miRNAs which targets them for degradation<sup>74</sup>. Given that both VSRs improve VSV $\Delta$ 51-mediated killing to the same extent, this suggests that globally blocking the RNAi pathway improves virus replication regardless of the mechanism through which this is achieved. It is also interesting to note that VP55 does not polyadenylate all small RNAs and key features such as the presence of a 2' O methyl group protect a subset of small RNAs from degradation<sup>74</sup>. Specifically, virally-derived siRNAs have been previously shown to be 2' O methylated, which protects them from degradation<sup>99</sup>. This may be especially advantageous for cell lines in which

direct viral genome cleavage occurs (T47D, HT29, SF295, MCF7 and HCT115) (Fig 3.10). Deep-sequencing of VSV $\Delta$ 51-VP55 infected cells could help to narrow down potential antiviral miRNAs given that VP55 degrades only a subset of small RNAs but gives similar results to VSV $\Delta$ 51-B2 infection.

#### **4.5 The interplay between B2 and the IFN response**

Given the importance of IFN signaling in mammalian antiviral defense, we investigated the potential impact of B2 on this response. B2 could potentially bind and sequester the dsRNA viral substrates and prevent PRR activation. Alternatively, B2 could protect miRNAs involved in downregulating expression of inducers of the IFN pathway, therefore resulting in a more robust activation of the IFN response in the presence of B2. This aligns with the counterintuitive finding that more IFN- $\beta$  was produced upon infection with the B2 virus compared to the parental virus (Fig 3.11, 3.12A, 3.12B). Although this is consistent with the presence of increased amounts of virus particles by the B2-expressing virus, one would expect an increased IFN production would correlate with decreased virus replication, which is the opposite of what we observe, suggesting that B2 expression is sufficient to overcome the robust antiviral response VSV-B2 induces. Also, pre-treatment of sensitive cell lines with IFN had a protective effect and reduced the improvement seen with VSV $\Delta$ 51-B2 infection (Fig 3.13A). Further to this, our vaccinia supernatant transfer experiments demonstrated that the blocking of Type I IFNs very minimally enhanced VSV $\Delta$ 51-B2 replication compared to VSV $\Delta$ 51-GFP (Fig 3.13B). This agrees with our B2 stable cell line data in which we demonstrated that WT VSV is not improved by B2 expression, suggesting that the ability to block IFN signaling does not further enhance VSV efficacy in the pres-

ence of B2 (Fig 3.2). Together this data suggests the IFN pathway is distinct and perhaps the dominant mechanism in controlling viral infection compared to anti-viral RNAi.

Despite this potential dominance of the IFN response, antiviral RNAi does appear to be important, at least for IFN deficient cells. It has been previously reported that exogenously supplied dsRNA can control the replication of both RNA and DNA viruses in cells with IFN defects<sup>100</sup>. In this study, the authors show that VSV replication can be significantly impaired in MEFs with deletions in the proteins IRF3 or IPS-1 downstream of IFN by pre-treatment with long dsRNA. Without pre-treatment, these deletions did not alter VSV replication compared to WT MEFs<sup>100</sup>. This suggests that dsRNA can elicit an antiviral response in the absence of Type I IFN signaling. This is in line with the idea that although the effect of IFN is dominant over the antiviral RNAi pathway in responsive cells, B2 does inhibit the antiviral response in a way that is at least partially independent from the IFN response.

Interestingly, despite the significantly higher levels of IFN- $\beta$  with VSV $\Delta$ 51-B2, we did not observe a corresponding increase in the ISGs OAS1 and MXA (Fig 3.12C). The influence of B2 on the transcription of downstream IFN genes is not something we have investigated thus far and perhaps could be an uncharacterized link between B2 and the IFN pathway in certain cell lines. Our B2 stable cell line would be a great tool to study this as a dose-response curve could be generated by treating with various doses of IFN and following with qPCR for ISGs. This would clarify whether the downstream IFN response is impaired or enhanced in the presence of B2.

#### **4.6 MicroRNAs and virus replication**

In addition to detecting viral siRNAs, we found that VSV $\Delta$ 51-B2 infection leads to changes in the total small RNA levels, which includes miRNAs, in certain cell lines (7860, M14,

T47D and SF295) (Fig 3.9). Notably, although VSV $\Delta$ 51-B2 shows impressive enhancement relative to VSV $\Delta$ 51-GFP in the M14 and 7860 cell lines, we did not detect direct viral genome cleavage. However, we did see a reduction in the 22-23nt peak in the total small RNA read length distributions in these cell lines, suggesting that perhaps B2 is blocking processing miRNAs, some of which could be antiviral. In some other cell lines, inhibition of both direct viral genome cleavage and antiviral miRNA seems to be occurring simultaneously. This interplay between viruses and host cell miRNAs is a concept that is supported by several studies. Firstly, knockdown of key proteins involved in the miRNA pathway has been shown to enhance the replication of a number of viruses. Dicer knockdown itself enhances the replication of a number of viruses which include both VSV and mouse cytomegalovirus (MCMV)<sup>101,102</sup>. Furthermore, while MCMV infection leads to the transcription of downstream IFN pathway genes like *Irf7* and *Oas7*<sup>101</sup>, the induction is reduced in dicer-deficient cells<sup>101</sup>. A similar mechanism could explain the results seen with VSV $\Delta$ 51-B2. Indeed, if B2 recapitulated the effects of Dicer-deficiency, VSV $\Delta$ 51-B2 infection could inhibit activation of innate antiviral pathways in cancers with remaining IFN responses. In fact, IFN has been shown to induce a number of miRNAs including *mir1*<sup>103-105</sup>, *mir129*<sup>106</sup>, *mir146*<sup>105</sup> and *mir155*<sup>105,107,108</sup>, some of which could have antiviral function. Looking further downstream the miRNA pathway, it has been previously demonstrated in HEK293 cells that PAMPs lead to inhibition of RISC<sup>98</sup>. Based on this data, an additional possibility is that binding of B2 to small RNAs could contribute synergistically with RISC inhibition to robustly block microRNA processing and function. Future studies investigating IFN-induced miRNAs and their targets should provide further direction to investigate this possibility.

As discussed above, miRNAs may regulate the activation of cellular anti-viral immunity. An additional possible mechanism would be the direct targeting of viral genomes or mRNA of

virally-encoded factors. Few examples of cellular miRNAs targeting specific viruses directly have already been described. One such example is mir-29 that has been reported to bind the 3' UTR of HIV mRNA and as a result sequesters the mRNA into processing bodies and inhibits its translation<sup>109</sup>. Also, IFN- $\beta$  induces various miRNAs that are complimentary to the hepatitis C virus (HCV) genomic RNA and inhibit viral replication<sup>104</sup>. Perhaps most relevant to our study, mir-24 and mir-93 have both been previously shown to directly target the VSV genome and limit VSV replication<sup>102</sup>. Importantly, our results show that VSV $\Delta$ 51-B2 infection leads to the down-regulation of both of these miRNAs, providing an additional explanation for the increased virus production using the B2 virus (Fig 3.8). It would be interesting to look into levels of mir-24 and mir-93 in our panel of cell lines to determine if elevated levels of these miRNAs correlates with increased sensitivity to VSV $\Delta$ 51-B2. In addition, it would be important to determine whether elevated levels of these miRNAs is specific to cancer or whether other normal tissues express similar levels and may pose a potential safety concern for the therapeutic use of VSV $\Delta$ 51-B2. Furthermore, as we have identified that B2 may alter microRNA production in certain cancer cell lines, it will be interesting to identify microRNAs which may have antiviral function and could be targeted to improve OV therapy. For example, microRNAs such as mir-24 and mir-93 which target VSV directly or other interesting candidates which may have broader antiviral effects. Identification of novel antiviral microRNAs would open the door to novel therapy combinations such as the combined administration of VSV $\Delta$ 51 and anti-miRs to sequester specific microRNAs which otherwise limit the efficacy of virus therapies.

#### 4.7 Dicer in cancer and infection

It is important to consider the impact of Dicer on OV efficacy as it plays an essential role in the generation of both mature siRNAs and miRNAs. Interestingly, shRNA knockdown of dicer has been shown to promote cellular transformation and enhance tumour growth in a K-Ras induced murine model of lung cancer<sup>110</sup>. This suggests that the inhibition of dicer may play a role in controlling tumorigenesis and its inhibition by B2 may have important repercussions beyond the simple enhancement of viral replication. Whether B2 interacts with dicer itself or could inhibit its function through an alternative mechanism is currently unknown. Our B2 stable cell line could be used to investigate this as co-immunoprecipitation of B2 could be used to determine if B2 and dicer interact. Additionally, mass spectrometry of B2 interacting partners could identify the entire interactome of B2 and reveal how its interactions with other proteins could affect dicer function. It is also interesting to note that elevated levels of Dicer are associated with a number of cancers<sup>111-113</sup>. One possibility could be that the cells in which VSVΔ51-B2 is most effective also have hyper-active or higher levels of Dicer. Interestingly, Flemr *et al* have shown that mouse and rat oocytes, but not somatic tissues, express an amino-terminally truncated isoform of Dicer that lacks its helicase domain which prevents dsRNA processing *in vitro*<sup>114</sup>. Unlike full-length dicer, this truncated form can process long dsRNA into siRNAs suggesting this isoform could facilitate a functioning RNAi pathway<sup>114</sup>. Although this isoform is described only in rodents thus far, the possibility that similar isoforms exist in other mammalian organisms is an avenue that remains to be explored. Given the genomic instability that characterizes many cancers<sup>115</sup>, it would be interesting to determine whether truncation mutations exist within the Dicer gene and whether these may affect dicer processing abilities.

#### **4.8 Implications for VSV $\Delta$ 51-B2 in cancer treatment**

It is well-established that OV<sub>s</sub> can be armed with tumor antigens for anti-cancer vaccination. Although direct oncolysis on its own releases tumor antigens, OV<sub>s</sub> encoding TAAs provide an extra edge as transgene expression is activated and amplified upon proficient viral infection within the confines of the tumor<sup>9</sup>. A myriad of OV vaccines have been designed for a number of viruses and antigens. For example, VSV $\Delta$ 51 encoding the antigen dopachrome tautomerase (DCT) enhances both CD4 and CD8 antigen-specific T cell responses and improves VSV efficacy in the B16F10 murine melanoma model<sup>116</sup>. Given that an antigen-specific immune response can be generated with antigen-encoding OV<sub>s</sub>, the enhanced replication imparted by B2 expression could further improve the robustness of this immune response. These OV vaccines should not only be even more robust immune-stimulators but additionally retain their safety profile as B2 enhances VSV replication in tumors but not in normal tissues (Fig 3.6B, 3.16). The concept of improving existing viral platforms through encoding B2 could also be used for OV<sub>s</sub> encoding cytokines or immune checkpoint inhibitors. Measles virus encoding CTLA-4 and PD-L1 as well as VSV $\Delta$ 51 encoding interferon gamma are just a few examples of such viruses<sup>41,117</sup>. The enhanced expression of these transgenes as a result of improved viral replication could further enhance therapeutic efficacy. Overall, the knowledge we gain from our study of VSV $\Delta$ 51-B2 should provide opportunity for the design of a wide array of novel OV<sub>s</sub> with enhanced therapeutic potential.

#### **4. Concluding Remarks**

In this study, we demonstrate a novel role of the RNAi pathway as an intrinsic antiviral mechanism in cancer cells and the potential of blocking RNAi to improve OV efficacy. Mechanistically, inhibition of direct viral genome cleavage as well as the modulation of miRNA processing both seem to be involved in enhancing VSV $\Delta$ 51 replication. This work provides insights into a novel mechanism of viral defense in cancer cells and promises to improve current OV therapies by tailoring viruses to overcome alternative antiviral mechanisms and be efficient in a broader range of cancers.

## References:

1. Postow, M. A., Callahan, M. K. & Wolchok, J. D. Immune Checkpoint Blockade in Cancer Therapy. *J. Clin. Oncol.* **33**, 1974–82 (2015).
2. Jackson, H. J., Rafiq, S. & Brentjens, R. J. Driving CAR T-cells forward. *Nat. Rev. Clin. Oncol.* **13**, 370–383 (2016).
3. Fesnak, A. D., June, C. H. & Levine, B. L. Engineered T cells: the promise and challenges of cancer immunotherapy. *Nat. Rev. Cancer* **16**, 566–581 (2016).
4. Guo, C. *et al.* Therapeutic cancer vaccines: past, present, and future. *Adv. Cancer Res.* **119**, 421–75 (2013).
5. Kaufman, H. L., Kohlhapp, F. J. & Zloza, A. Oncolytic viruses: a new class of immunotherapy drugs. *Nat. Rev. Drug Discov.* **14**, 642–662 (2015).
6. Lichty, B. D., Breitbach, C. J., Stojdl, D. F. & Bell, J. C. Going viral with cancer immunotherapy. *Nat. Rev. Cancer* **14**, 559–67 (2014).
7. Lin, E. & Nemunaitis, J. Oncolytic viral therapies. *Cancer Gene Ther.* **11**, 643–664 (2004).
8. Liu, T.-C., Galanis, E. & Kirn, D. Clinical trial results with oncolytic virotherapy: a century of promise, a decade of progress. *Nat Clin Pract Oncol.* **4**, 101-117 (2007).
9. Aitken, A., Roy, D. & Bourgeois-Daigneault, M.-C. Taking a Stab at Cancer; Oncolytic Virus-Mediated Anti-Cancer Vaccination Strategies. *Biomedicines* **5**, 3 (2017).
10. Bastin, D., Walsh, S., Al Saigh, M. & Wan, Y. Capitalizing on Cancer Specific Replication: Oncolytic Viruses as a Versatile Platform for the Enhancement of Cancer Immunotherapy Strategies. *Biomedicines* **4**, 21 (2016).
11. Breitbach, C. J., Moon, A., Burke, J., Hwang, T.-H. & Kirn, D. H. A Phase 2, Open-Label,

- Randomized Study of Pexa-Vec (JX-594) Administered by Intratumoral Injection in Patients with Unresectable Primary Hepatocellular Carcinoma. *Methods Mol Bio.* **1317**, 343–357 (2015).
12. Heo, J. *et al.* Randomized dose-finding clinical trial of oncolytic immunotherapeutic vaccinia JX-594 in liver cancer. *Nat. Med.* **19**, 329–336 (2013).
  13. Arulanandam, R. *et al.* VEGF-Mediated Induction of PRD1-BF1/Blimp1 Expression Sensitizes Tumor Vasculature to Oncolytic Virus Infection. *Cancer Cell* **28**, 210–224 (2015).
  14. Melcher, A., Parato, K., Rooney, C. M. & Bell, J. C. Thunder and lightning: immunotherapy and oncolytic viruses collide. *Mol. Ther.* **19**, 1008–16 (2011).
  15. Ivashkiv, L. B. & Donlin, L. T. Regulation of type I interferon responses. *Nat. Rev. Immunol.* **14**, 36–49 (2014).
  16. Rieder, M. & Conzelmann, K. . Rhabdovirus evasion of the interferon system. *J Interf. Cytokine Res* **29**, 499–510 (2009).
  17. Staeheli, P. & Pavlovic, J. Inhibition of vesicular stomatitis virus mRNA synthesis by human MxA protein. *J. Virol.* **65**, 4498–501 (1991).
  18. Krishnamoorthy, J., Mounir, Z., Raven, J. & Koromilas, A. The eIF2 $\alpha$  kinases inhibit vesicular stomatitis virus replication independently of eIF2 phosphorylation. *Cell Cycle* **7**, 2346–2351 (2008).
  19. Weidner, J. M. *et al.* Interferon-induced cell membrane proteins, IFITM3 and tetherin, inhibit vesicular stomatitis virus infection via distinct mechanisms. *J. Virol.* **84**, 12646–57 (2010).
  20. Ilkow, C. S., Swift, S. L., Bell, J. C. & Diallo, J.-S. From scourge to cure: tumour-

- selective viral pathogenesis as a new strategy against cancer. *PLoS Pathog.* **10**, e1003836 (2014).
21. Dunn, G. P., Koebel, C. M. & Schreiber, R. D. Interferons, immunity and cancer immunoediting. *Nat. Rev. Immunol.* **6**, 836–848 (2006).
  22. Muñoz-Fontela, C. *et al.* p53 serves as a host antiviral factor that enhances innate and adaptive immune responses to influenza A virus. *J. Immunol.* **187**, 6428–36 (2011).
  23. Nguyen, M. L. *et al.* p53 and hTERT determine sensitivity to viral apoptosis. *J. Virol.* **81**, 12985–95 (2007).
  24. Garcia, M. A. *et al.* Activation of NF-kB pathway by virus infection requires Rb expression. *PLoS One* **4**, e6422 (2009).
  25. Zheng, Y., Stamminger, T., Hearing, P., Dieterle, A. & Pavirani, A. E2F/Rb Family Proteins Mediate Interferon Induced Repression of Adenovirus Immediate Early Transcription to Promote Persistent Viral Infection. *PLOS Pathog.* **12**, e1005415 (2016).
  26. Sherr, C. J. & McCormick, F. The RB and p53 pathways in cancer. *Cancer Cell* **2**, 103–112 (2002).
  27. Fields, B. N., Knipe, D. M., & Howley, P. M. *Fields Virology*. (Lippincott Williams & Wilkins, 2007).
  28. Hastie, E. & Grdzlishvili, V. Z. Vesicular stomatitis virus as a flexible platform for oncolytic virotherapy against cancer. *J. Gen. Virol.* **93**, 2529–2545 (2012).
  29. Kurisetty, V. V. S. *et al.* Preclinical safety and activity of recombinant VSV-IFN- $\beta$  in an immunocompetent model of squamous cell carcinoma of the head and neck. *Head Neck* **36**, 1619–27 (2014).
  30. Ball, L. A., Pringle, C. R., Flanagan, B., Perepelitsa, V. P. & Wertz, G. W. Phenotypic

- consequences of rearranging the P, M, and G genes of vesicular stomatitis virus. *J. Virol.* **73**, 4705–12 (1999).
31. Black, B. L. & Lyles, D. S. Vesicular stomatitis virus matrix protein inhibits host cell-directed transcription of target genes in vivo. *J. Virol.* **66**, 4058–64 (1992).
  32. Ahmed, M. & Lyles, D. S. Effect of vesicular stomatitis virus matrix protein on transcription directed by host RNA polymerases I, II, and III. *J. Virol.* **72**, 8413–9 (1998).
  33. Petersen, J. M., Her, L. S., Varvel, V., Lund, E. & Dahlberg, J. E. The matrix protein of vesicular stomatitis virus inhibits nucleocytoplasmic transport when it is in the nucleus and associated with nuclear pore complexes. *Mol. Cell. Biol.* **20**, 8590–601 (2000).
  34. Terstegen, L. *et al.* The Vesicular Stomatitis Virus Matrix Protein Inhibits Glycoprotein 130-Dependent STAT Activation. *J. Immunol.* **167**, 5209-5216 (2001).
  35. Stojdl, D. F. *et al.* VSV strains with defects in their ability to shutdown innate immunity are potent systemic anti-cancer agents. *Cancer Cell* **4**, 263–75 (2003).
  36. Stojdl DF, Lichty B, Knowles S, Marius R, Atkins H, Sonenberg N, B. J. Exploiting tumor-specific defects in the interferon pathway with a previously unknown oncolytic virus. *Nature Medicine* **6**, 821–825 (2000).
  37. Barnes, D., Kunitomi, M., Vignuzzi, M., Saksela, K. & Andino, R. Harnessing endogenous miRNAs to control virus tissue tropism as a strategy for developing attenuated virus vaccines. *Cell Host Microbe* **4**, 239–48 (2008).
  38. Johnson, J. E. *et al.* Neurovirulence properties of recombinant vesicular stomatitis virus vectors in non-human primates. *Virology* **360**, 36–49 (2007).
  39. Huneycutt, B. S. *et al.* Distribution of vesicular stomatitis virus proteins in the brains of BALB/c mice following intranasal inoculation: an immunohistochemical analysis. *Brain*

- Res.* **635**, 81–95 (1994).
40. Kelly, E. J., Nace, R., Barber, G. N. & Russell, S. J. Attenuation of VSV-encephalitis through microRNA-targeting. *J. Virol* **84**, 1550-1562 (2009).
  41. Bourgeois-Daigneault, M.-C. *et al.* Oncolytic vesicular stomatitis virus expressing interferon- $\gamma$  has enhanced therapeutic activity. *Mol Ther Oncolytics* **3**, e16001 (2016).
  42. Yu, F. *et al.* T-cell Engager-armed Oncolytic Vaccinia Virus Significantly Enhances Antitumor Therapy. *Mol. Ther.* **22**, 102–111 (2014).
  43. Du, T. *et al.* Tumor-specific oncolytic adenoviruses expressing granulocyte macrophage colony-stimulating factor or anti-CTLA4 antibody for the treatment of cancers. *Cancer Gene Ther.* **21**, 340–8 (2014).
  44. Li, J. *et al.* Chemokine expression from oncolytic vaccinia virus enhances vaccine therapies of cancer. *Mol. Ther.* **19**, 650–7 (2011).
  45. Msaouel, P. *et al.* Engineered Measles Virus as a Novel Oncolytic Therapy Against Prostate Cancer. *Prostate.* **1**, 82–91 (2009).
  46. Rommelfanger, D. M. *et al.* Systemic combination virotherapy for melanoma with tumor antigen-expressing vesicular stomatitis virus and adoptive T-cell transfer. *Cancer Res.* **72**, 4753–64 (2012).
  47. Peng, K.-W. *et al.* Intraperitoneal Therapy of Ovarian Cancer Using an Engineered Measles Virus. *Cancer Res.* **62**, 4656–4662 (2002).
  48. Wassenegger, M. The Role of the RNAi Machinery in Heterochromatin Formation. *Cell* **122**, 13–16 (2005).
  49. Obbard, D. J., Gordon, K. H. J., Buck, A. H. & Jiggins, F. M. The evolution of RNAi as a defence against viruses and transposable elements. *Philos. Trans. R. Soc. Lond. B. Biol.*

- Sci.* **364**, 99–115 (2009).
50. Ding, S.-W. & Voinnet, O. Antiviral immunity directed by small RNAs. *Cell* **130**, 413–26 (2007).
  51. Fire A, Xu S, Montgomery MK, Kostas SA, Driver SE, M. C. Potent and specific genetic interference by double-stranded RNA in *Caenorhabditis elegans*. *Nat.* **391**, 806–811 (1998).
  52. Ghildiyal, M. & Zamore, P. D. Small silencing RNAs: an expanding universe. *Nat. Rev. Genet.* **10**, 94–108 (2009).
  53. Winter, J., Jung, S., Keller, S., Gregory, R. I. & Diederichs, S. Many roads to maturity: microRNA biogenesis pathways and their regulation. *Nat. Cell Biol.* **11**, 228–234 (2009).
  54. Bartel, D. P. MicroRNAs: Genomics, Biogenesis, Mechanism and Function. *Cell* **116**, 281–297 (2004).
  55. Kim, V. N., Han, J. & Siomi, M. C. Biogenesis of small RNAs in animals. *Nat Rev Mol Cell Biol* **10**, 126–139 (2009).
  56. Hutvagner, G. & Simard, M. J. Argonaute proteins: key players in RNA silencing. *Nat. Rev. Mol. Cell Biol.* **9**, 22–32 (2008).
  57. Diederichs, S. *et al.* Dual role for argonautes in microRNA processing and posttranscriptional regulation of microRNA expression. *Cell* **131**, 1097–108 (2007).
  58. Gantier, M. P. & Williams, B. R. G. The response of mammalian cells to double-stranded RNA. *Cytokine Growth Factor Rev.* **18**, 363–71 (2007).
  59. Voinnet, O. Induction and suppression of RNA silencing: insights from viral infections. *Nat. Rev. Genet.* **6**, 206–220 (2005).
  60. Jiang, L., Wei, C. & Li, Y. Viral suppression of RNA silencing. *Sci. China. Life Sci.* **55**,

- 109–18 (2012).
61. Silhavy, D. *et al.* A viral protein suppresses RNA silencing and binds silencing-generated, 21- to 25-nucleotide double-stranded RNAs. *EMBO J.* **21**, 3070–80 (2002).
  62. Csorba, T., Lózsa, R., Hutvágner, G. & Burgyán, J. Poliovirus protein P0 prevents the assembly of small RNA-containing RISC complexes and leads to degradation of ARGONAUTE1. *Plant J.* **62**, 463–472 (2010).
  63. Johnson, K. L., Price, B. D., Eckerle, L. D. & Ball, L. A. Nodamura Virus Nonstructural Protein B2 Can Enhance Viral RNA Accumulation in both Mammalian and Insect Cells. *J. Virol.* **78**, 6698–6704 (2004).
  64. Bailey, L., Newman, J. F. & Porterfield, J. S. The multiplication of Nodamura virus in insect and mammalian cell cultures. *J. Gen. Virol.* **26**, 15–20 (1975).
  65. Bailey, L. & Scott, H. A. The pathogenicity of Nodamura virus for insects. *Nature* **241**, 545 (1973).
  66. Chao, J. A. *et al.* Dual modes of RNA-silencing suppression by Flock House virus protein B2. *Nat. Struct. Mol. Biol.* **12**, 952–957 (2005).
  67. Kingsolver, M. B., Huang, Z. & Hardy, R. W. Insect antiviral innate immunity: pathways, effectors, and connections. *J. Mol. Biol.* **425**, 4921–36 (2013).
  68. Lu, Y., Wambach, M., Katze, M. G. & Krug, R. M. Binding of the influenza virus NS1 protein to double-stranded RNA inhibits the activation of the protein kinase that phosphorylates the eIF-2 translation initiation factor. *Virology* **214**, 222–8 (1995).
  69. Bucher, E., Hemmes, H., de Haan, P., Goldbach, R. & Prins, M. The influenza A virus NS1 protein binds small interfering RNAs and suppresses RNA silencing in plants. *J. Gen. Virol.* **85**, 983–91 (2004).

70. Cárdenas, W. B. *et al.* Ebola virus VP35 protein binds double-stranded RNA and inhibits alpha/beta interferon production induced by RIG-I signaling. *J. Virol.* **80**, 5168–78 (2006).
71. Haasnoot, J. *et al.* The Ebola Virus VP35 Protein Is a Suppressor of RNA Silencing. *PLoS Pathog.* **3**, e86 (2007).
72. Bennasser, Y., Le, S.-Y., Benkirane, M. & Jeang, K.-T. Evidence that HIV-1 Encodes an siRNA and a Suppressor of RNA Silencing. *Immunity* **22**, 607–619 (2005).
73. Bennasser, Y. & Jeang, K.-T. HIV-1 Tat interaction with Dicer: requirement for RNA. *Retrovirology* **3**, 95 (2006).
74. Backes, S. *et al.* Degradation of host MicroRNAs by poxvirus poly(A) polymerase reveals terminal RNA methylation as a protective antiviral mechanism. *Cell Host Microbe* **12**, 200–210 (2012).
75. Paddison, P. J., Caudy, A. A., Hannon, G. J. & Hannon, G. J. Stable Suppression of Gene Expression by RNAi in Mammalian Cells. *Proc Natl Acad Sci USA.* **99**, 1443–1448 (2002).
76. Parameswaran, P. *et al.* Six RNA Viruses and Forty-One Hosts: Viral Small RNAs and Modulation of Small RNA Repertoires in Vertebrate and Invertebrate Systems. *PLoS Pathog.* **6**, e1000764 (2010).
77. Nejepinska, J. *et al.* dsRNA expression in the mouse elicits RNAi in oocytes and low adenosine deamination in somatic cells. *Nucleic Acids Res.* **40**, 399–413 (2012).
78. Maillard, P. V *et al.* Antiviral RNA interference in mammalian cells. *Science.* **342**, 235–238 (2013).
79. Li, Y., Lu, J., Han, Y., Fan, X. & Ding, S. W. RNA interference functions as an antiviral immunity mechanism in mammals. *Science.* **342**, 231–234 (2013).

80. Chen, L.-L., Yang, L. & Carmichael, G. G. Molecular basis for an attenuated cytoplasmic dsRNA response in human embryonic stem cells. *Cell Cycle* **9**, 3552–64 (2010).
81. Ben-Porath, I. *et al.* An embryonic stem cell-like gene expression signature in poorly differentiated aggressive human tumors. *Nat Genet* **40**, 499–507 (2008).
82. Somervaille, T. C. P. *et al.* Hierarchical Maintenance of MLL Myeloid Leukemia Stem Cells Employs a Transcriptional Program Shared with Embryonic Rather Than Adult Stem Cells. *Cell Stem Cell* **4**, 129–140 (2009).
83. Schoenhals, M. *et al.* Embryonic stem cell markers expression in cancers. *Biochem. Biophys. Res. Commun.* **383**, 157–162 (2009).
84. Mizuno, H., Spike, B. T., Wahl, G. M. & Levine, A. J. Inactivation of p53 in breast cancers correlates with stem cell transcriptional signatures. *Proc. Natl. Acad. Sci.* **107**, 22745–22750 (2010).
85. Sullivan, C. S. & Ganem, D. A virus-encoded inhibitor that blocks RNA interference in mammalian cells. *J. Virol.* **79**, 7371–9 (2005).
86. Lawson, N. D., Stillman, E. A., Whitt, M. A. & Rose, J. K. Recombinant vesicular stomatitis viruses from DNA. *Proc. Natl. Acad. Sci. U. S. A.* **92**, 4477–81 (1995).
87. Roy, D. G. *et al.* Programmable insect cell carriers for systemic delivery of integrated cancer biotherapy. *J. Control. Release* **220**, 210–21 (2015).
88. Le Boeuf, F. *et al.* Synergistic interaction between oncolytic viruses augments tumor killing. *Mol. Ther.* **18**, 888–95 (2010).
89. Svoboda, P. Selected reduction of dormant maternal mRNAs in mouse oocytes by RNA interference. *Dev.* **127**, 4147–4156 (2000).
90. Swartzendruberzj, D. E. & Lehman, J. M. Neoplastic Differentiation: Interaction of

- Simian Virus 40 and Polyoma Virus with Murine Teratocarcinoma Cells In Vitro. *J Cell Physiol.* **85**, 179-187 (1975).
91. Billy, E., Brondani, V., Zhang, H., Mü, U. & Filipowicz, W. Specific interference with gene expression induced by long, double-stranded RNA in mouse embryonal teratocarcinoma cell lines. *Proc Natl Acad Sci USA.* **98**, 14428-33 (2001).
  92. Blakqori, G. *et al.* La Crosse bunyavirus nonstructural protein NSs serves to suppress the type I interferon system of mammalian hosts. *J. Virol.* **81**, 4991–9 (2007).
  93. Wang, R. *et al.* Mouse embryonic stem cells are deficient in type I interferon expression in response to viral infections and double-stranded RNA. *J. Biol. Chem.* **288**, 15926–36 (2013).
  94. Haines, G. K. *et al.* Expression of the double-stranded RNA-dependent protein kinase (p68) in human breast tissues. *Tumour Biol.* **17**, 5–12 (1996).
  95. Pataer, A. *et al.* Prognostic significance of RNA-dependent protein kinase on non-small cell lung cancer patients. *Clin. Cancer Res.* **16**, 5522–8 (2010).
  96. Haines, G. K. *et al.* Correlation of the expression of double-stranded RNA-dependent protein kinase (p68) with differentiation in head and neck squamous cell carcinoma. *Virchows Arch. B. Cell Pathol. Incl. Mol. Pathol.* **63**, 289–95 (1993).
  97. Li, Y. *et al.* Induction and suppression of antiviral RNA interference by influenza A virus in mammalian cells. *Nat. Microbiol.* **2**, 16250 (2016).
  98. Seo, G. J. *et al.* Reciprocal inhibition between intracellular antiviral signaling and the RNAi machinery in mammalian cells. *Cell Host Microbe* **14**, 435–45 (2013).
  99. Daffis, S. *et al.* 2'-O methylation of the viral mRNA cap evades host restriction by IFIT family members. *Nature* **468**, 452–6 (2010).

100. DeWitte-Orr, S. J. *et al.* Long double-stranded RNA induces an antiviral response independent of IFN regulatory factor 3, IFN-beta promoter stimulator 1, and IFN. *J. Immunol.* **183**, 6545–53 (2009).
101. Ostermann, E. *et al.* Deregulation of type I IFN-dependent genes correlates with increased susceptibility to cytomegalovirus acute infection of dicer mutant mice. *PLoS One* **7**, e43744 (2012).
102. Otsuka, M. *et al.* Hypersusceptibility to Vesicular Stomatitis Virus Infection in Dicer1-Deficient Mice Is Due to Impaired miR24 and miR93 Expression. *Immunity* **27**, 123–134 (2007).
103. Scagnolari, C. *et al.* Differential expression of interferon-induced microRNAs in patients with chronic hepatitis C virus infection treated with pegylated interferon alpha. *Virology* **7**, 311 (2010).
104. Pedersen, I. M. *et al.* Interferon modulation of cellular microRNAs as an antiviral mechanism. *Nature* **449**, 919–22 (2007).
105. Bruni, R. *et al.* An integrated approach identifies IFN-regulated microRNAs and targeted mRNAs modulated by different HCV replicon clones. *BMC Genomics* **12**, 485 (2011).
106. Zhang, J. *et al.* Interferon- $\beta$  induced microRNA-129-5p down-regulates HPV-18 E6 and E7 viral gene expression by targeting SP1 in cervical cancer cells. *PLoS One* **8**, e81366 (2013).
107. Zhang, J. *et al.* Interferon- $\beta$ -induced miR-155 inhibits osteoclast differentiation by targeting SOCS1 and MITF. *FEBS Lett.* **586**, 3255–3262 (2012).
108. O’Connell, R. M., Taganov, K. D., Boldin, M. P., Cheng, G. & Baltimore, D. MicroRNA-155 is induced during the macrophage inflammatory response. *Proc. Natl. Acad. Sci. U. S.*

- A.* **104**, 1604–9 (2007).
109. Nathans, R. *et al.* Cellular microRNA and P bodies modulate host-HIV-1 interactions. *Mol. Cell* **34**, 696–709 (2009).
  110. Kumar, M. S., Lu, J., Mercer, K. L., Golub, T. R. & Jacks, T. Impaired microRNA processing enhances cellular transformation and tumorigenesis. *Nat. Genet.* **39**, 673–677 (2007).
  111. Chiosea, S. *et al.* Overexpression of Dicer in Precursor Lesions of Lung Adenocarcinoma. *Cancer Res.* **67**, 2345–2350 (2007).
  112. Martin, M. G., Payton, J. E. & Link, D. C. Dicer and outcomes in patients with acute myeloid leukemia (AML). *Leuk. Res.* **33**, e127 (2009).
  113. Jakymiw, A. *et al.* Overexpression of dicer as a result of reduced let-7 MicroRNA levels contributes to increased cell proliferation of oral cancer cells. *Genes, Chromosom. Cancer* **49**, 549–559 (2010).
  114. Flemr, M. *et al.* A Retrotransposon-Driven Dicer Isoform Directs Endogenous Small Interfering RNA Production in Mouse Oocytes. *Cell* **155**, 807–816 (2013).
  115. Hanahan, D. & Weinberg, R. A. Hallmarks of cancer: The next generation. *Cell* **144**, 646–674 (2011).
  116. Bridle, B. W. *et al.* Vesicular stomatitis virus as a novel cancer vaccine vector to prime antitumor immunity amenable to rapid boosting with adenovirus. *Mol Ther* **17**, 1814–1821 (2009).
  117. Engeland, C. E. *et al.* CTLA-4 and PD-L1 checkpoint blockade enhances oncolytic measles virus therapy. *Mol. Ther.* **22**, 1949–59 (2014).

# Curriculum Vitae

## Education

- 2015-2017**    **Master of Science in Biochemistry**  
**Specialization in Human and Molecular Genetics**  
Department of Biochemistry, Microbiology and Immunology  
University of Ottawa, Ottawa, Ontario  
**Thesis (2015-2017):** Blocking the RNA interference pathway improves oncolytic virus therapy  
**Supervisor:** Dr. John Bell
- 2016**        **Introduction to R & Exploratory Analysis of Biological Data using R.**  
*Canadian Bioinformatics Workshops.*  
Toronto ON.
- 2011- 2015**    **Bachelor of Medical Science (B.M.Sc)**  
**Honours Specialization in Biochemistry**  
Department of Biochemistry  
University of Western Ontario, London, Ontario  
**Thesis (2014-2015):** Characterizing the interaction between the DNA double-stranded break repair protein Ku70 and Aurora B kinase  
**Supervisor:** Dr. Caroline Schild-Poulter

## Research Experience

- 2015 – 2017**        **Centre for Innovative Cancer Research**  
Ottawa Hospital Research Institute, Ottawa, Ontario
- Graduate work, Department of Biochemistry, University of Ottawa
  - Developed and characterize the molecular mechanism of a novel oncolytic virus
  - Supervisor: Dr. John Bell
- 2014-2015**        **Robarts Research Institute**  
University of Western Ontario, London Ontario
- Undergraduate thesis work, Department of Biochemistry, University of Western Ontario
  - Investigating the interaction between the DNA double-strand repair protein Ku70 and a novel interacting kinase protein Aurora B
  - Supervisor: Dr. Caroline Schild-Poulter

- 2014**                    **Robarts Research Institute**  
University of Western Ontario, London Ontario
- Undergraduate NSERC USRA, Department of Biochemistry, University of Western Ontario
  - Investigating the interaction between the DNA double-strand repair protein Ku70 and a novel interacting kinase protein Aurora B
- 2013**                    **Agriculture and Agri-Food Canada**  
University of Western Ontario, London Ontario
- Undergraduate NSERC USRA, Department of Biology, University of Western Ontario
  - Characterizing the GmMY176 interactome and its role in soybean isoflavonoid biosynthesis
  - Supervisor: Sangeeta Dhaubhadel
- 2011-2013**            **University of Western Ontario**  
London Ontario
- Undergraduate volunteer, Department of Biology, University of Western Ontario
  - Drosophila melongaster propagation and breeding
  - Supervisor: Dr. Anthony Percival-Smith

## **Awards**

- 2017**                    **Syed Sattar MSc Student Award (\$500)**  
University of Ottawa, Ottawa, Ontario
- 2016**                    **Ottawa Hospital Research Day 1<sup>st</sup> place oral presentation (\$500)**  
Ottawa, Ontario
- 2015**                    **Gold Medalist, Honours Specialization Biochemistry**  
University of Western Ontario, London, Ontario
- 2011-2015**            **University of Western Ontario Honour Roll**  
University of Western Ontario, London, Ontario
- 2014**                    **NSERC Undergraduate Summer Research Award (\$6000)**  
University of Western Ontario, London, Ontario
- 2013**                    **NSERC Undergraduate Summer Research Award (\$6000)**  
University of Western Ontario, London, Ontario

## Scholarships

- 2016-2017**      **Ontario Graduate Scholarship** (\$15,000)  
University of Ottawa, Ottawa, Ontario
- 2015-2016**      **NSERC CGS-M** (\$17, 500)  
University of Ottawa, Ottawa, Ontario
- 2015-2016**      **Ontario Graduate Scholarship** (\$15,000) (Declined)  
University of Western Ontario, London, Ontario
- 2011-2015**      **UWO Continuing Admission Scholarship** (\$2500 annually)  
University of Western Ontario, London, Ontario
- 2011-2015**      **Queen Elizabeth Aiming for the Top Scholarship** (\$200 annually)  
University of Western Ontario, London, Ontario
- 2014**              **Dr. G. E. Hall Scholarship** (\$500)  
University of Western Ontario, London, Ontario
- 2013-2015**      **Royal Canadian Legion A.V.M Sully Branch 109 Scholarship** (\$1000  
annually)

## Published Articles

**Aitken A**, Roy DG, Bell J & Bourgeois-Daigneault M. 2017. *Taking a Stab at Cancer; Oncolytic Virus-Mediated Anti-Cancer Vaccination Strategies*. Biomedicines.

Fell V, Walden E, Hoffer S, Rogers S, **Aitken A**, Salemi L & Schild-Poulter C. 2016. *Ku70 phosphorylation mediates Aurora B inhibition and activation of the DNA damage response*. Nature Scientific Reports.

Bourgeois-Daigneault M, St-Germain L, Roy DG, Pelin A, **Aitken A**, Arulanandam R, Falls T, Garcia V, Diallo JS, Bell JC. 2016. *Combination of Paclitaxel and MGI oncolytic virus as a successful strategy for breast cancer treatment*. Breast Cancer Research.

## Articles in Preparation

Neo-Adjuvant Oncolytic Virotherapy Prior to Surgery Sensitizes Triple-Negative Breast Cancer to Immune Checkpoint Therapy. M.-C. Bourgeois-Daigneault, D. G. Roy, **A. S. Aitken**, T. Falls, L. E. St-Germain, A. Pelin, B. D. Lichty, D. F. Stojdl, G. Ungerechts, J. C. Bell.

Brief Communication; A Heterologous Oncolytic Bacteria-Virus Prime-Boost Approach for Anti-Cancer Vaccination. **Amelia Sadie Aitken**, Dominic Guy Roy, John Cameron Bell and Marie-Claude Bourgeois-Daigneault.

Blocking the RNA interference pathway improves oncolytic virus therapy. **Aitken A.**, Bastin D., Pelin A., Roy D.G., Pikor L., Huh M., Bourgeois-Daigneault MC., Bell J.C., and Ilkow C.

## Conferences

### *Poster presentations*

**Amelia Aitken**, Carolina Ilkow, Donald Bastin, Adrian Pelin, John Bell. Characterizing the molecular and immune response to an oncolytic virus targeting the RNAi pathway. *Terry Fox Research Institute Annual Conference*. Vancouver BC. May 2016

**Amelia Aitken**, Carolina Ilkow, Donald Bastin, Adrian Pelin, John Bell. Characterizing the molecular and immune response to an oncolytic virus targeting the RNAi pathway. *BioCanRx Cancer Immunotherapy Conference*. Halifax NS. June 2016

**Amelia Aitken**, Donald Bastin, Mike Huh, Dominic Roy, Marie-Claude Bourgeois- Daigneault, Adrian Pelin, Larissa Pikor, John Bell, Carolina Ilkow. The molecular and immune response to an oncolytic virus targeting the RNAi pathway. *Keystone Symposium: Immune Regulation in Autoimmunity and Cancer*. Whistler BC. March 2017)

### *Oral presentations*

**Amelia Aitken**, Carolina Ilkow, Donald Bastin, Adrian Pelin, John Bell. Characterizing the molecular and immune response to an oncolytic virus targeting the RNAi pathway. *Terry Fox Research Institute Annual Conference*. Vancouver BC. May 2016

**Amelia Aitken**, Donald Bastin, Mike Huh, Dominic Roy, Marie-Claude Bourgeois- Daigneault, Adrian Pelin, Larissa Pikor, John Bell, Carolina Ilkow. An oncolytic virus targeting the RNA interference pathway. *10<sup>th</sup> Annual International Meeting on Replicating Oncolytic Virus Therapeutics*. Vancouver BC. October 2016

**Amelia Aitken**, Donald Bastin, Mike Huh, Dominic Roy, Marie-Claude Bourgeois- Daigneault, Adrian Pelin, Larissa Pikor, John Bell, Carolina Ilkow. An oncolytic virus targeting the RNA interference pathway. *Ottawa Hospital Research Day*. Ottawa ON. November 2016

**Amelia Aitken**, Donald Bastin, Mike Huh, Dominic Roy, Marie-Claude Bourgeois- Daigneault, Adrian Pelin, Larissa Pikor, John Bell, Carolina Ilkow. Blocking the RNA interference pathway improves oncolytic virus therapy. *University of Ottawa Bio-X Research Connections Conference*. Ottawa ON. March 2017

**Amelia Aitken**, Donald Bastin, Mike Huh, Dominic Roy, Marie-Claude Bourgeois- Daigneault, Adrian Pelin, Larissa Pikor, John Bell, Carolina Ilkow. Blocking the RNA interference pathway improves oncolytic virus therapy. *Department of Biochemistry, Microbiology and Immunology Research Day*. Ottawa ON. March 2017

## **Volunteer Experience**

2015-2017 **Let's Talk Science**, Ottawa ON  
2015-2016 **Ottawa Ronald McDonald House**, Ottawa ON  
2013-2015 **Rowntree United Soup Kitchen**, London ON  
2013-2014 **Canadian Blood Services and OneMatch Stem Cell Registry**, London ON  
2011-2013 **Dr. Anthony Percival Smith Molecular Biology Lab**, London ON